J. Fluid Mech. (1979), *vol.* 91, *part* 4, *pp.* 601–632
Printed in Great Britain

Scattering and distortion of the unsteady motion on transversely sheared mean flows

By M. E. GOLDSTEIN
NASA Lewis Research Center, Cleveland, Ohio 44135

(Received 28 March 1978 and in revised form 22 June 1978)

It is shown that the pressure and velocity fluctuations of the unsteady motion on a transversely sheared mean flow can be expressed entirely in terms of the derivatives of two potential functions. One of these is a convected quantity (i.e. it is frozen in the flow) that can be specified as a boundary condition and is related to a transverse component of the upstream velocity field. The other can be determined by solving an inhomogeneous wave equation whose source term is also a convected quantity that can be specified as a boundary condition in any given problem. The latter is related to the curl of the upstream vorticity field. The results are used to obtain an explicit representation of the three-dimensional gust-like or hydrodynamic motion on a transversely sheared mean flow. It is thereby shown that this motion is 'driven' entirely by the two convected quantities alluded to above.

The general theory is used to study the interaction of an unsteady flow with a semi-infinite plate embedded in a shear layer. The acoustic field produced by this interaction is calculated in the limits of low and high frequency. The results are compared with experimental one-third octave sound pressure level radiation patterns. The agreement is found to be excellent, especially in the low frequency range, where the mean-flow and convective effects are shown to have a strong influence on the directivity of the sound.

1. Introduction

The nature of the small amplitude unsteady motion imposed on a uniform (i.e. constant velocity) compressible flow is now well understood (Kovásznay 1953). In such a flow the velocity field can be decomposed into the sum of (i) a disturbance (often called a gust) that is purely convected (i.e. is frozen in the flow), has zero divergence and is completely decoupled from the fluctuations in pressure or any other thermodynamic property and (ii) an irrotational disturbance that produces no entropy fluctuations but is directly related to the pressure fluctuations and is, as a result, connected with any acoustic or other 'potential' type motion that may occur. Each of these types of disturbance is itself a solution to the governing equations and can therefore be imposed on the flow independently of the other.

Over the years, this decomposition has proved extremely useful for the formulation of problems that involve the interaction of small amplitude upstream distortions with airfoils and other aerodynamic surfaces. For example, the well-known Sears (1941) function describes the response of a two-dimensional airfoil to a two-dimensional convected gust for the case where the flow is incompressible. Since this result appeared many such response functions or in most cases their numerical equivalents have been

0022–1120/79/4176–6130 $02.00

deduced. These extensions include compressibility effects and account for three-dimensional convected disturbances (see Goldstein 1976, pp. 136–139 for a summary).

The response functions have been used to calculate the buffeting of an airfoil due to atmospheric turbulence (Liepmann 1952) and the radiated sound fields and unsteady aerodynamic loads caused by both steady and turbulent non-uniform flows interacting with propellers, helicopter rotors and aircraft engine fans and compressors.

The Kovásznay (1953) decomposition owes its great utility to two properties of the convected vortical solutions. First, such solutions can exist and remain finite everywhere in the flow even when there are no bounding surfaces present. They can therefore be used to represent an incident disturbance that would exist when the interacting surfaces were not present, i.e. a disturbance field that can be imposed on the flow independently of any boundary surfaces that may be present. Second, they provide a good representation of the actual non-uniform flows that are encountered in practice, including, as a result of Taylor's hypothesis, flows with upstream turbulence.

There are, however, many cases in which the mean flow cannot be treated as being uniform but rather contains substantial transverse velocity gradients. Such flows occur in the vicinity of the tail surfaces in conventional aircraft but are even more prominent in V/STOL aircraft, where the jet exhaust streams are deliberately made to interact with wings, flaps and other surfaces. Consequently, it is necessary to account for transverse velocity gradients when calculating the unsteady aerodynamic loads and resulting sound fields produced by the turbulence in such flows.

In a recent paper (hereafter referred to as I) Goldstein (1978) showed how the convected gust solutions for a uniform mean flow can be generalized to the case where the unsteady motion is imposed on a transversely sheared mean flow. This was done in a way that allows the generalized gust to represent unsteady incident disturbances on transversely sheared mean flows in the manner in which the Kovásznay (1953) solutions have been used to represent them on uniform flows.

A transversely sheared flow is one in which the velocity has the same direction at every point of the flow but can vary in magnitude along any line perpendicular to that direction. If such a flow is steady it will satisfy the inviscid non-heat-conducting equations of motion as long as we require that (i) the pressure be everywhere constant and that (ii) the density remains constant on the surfaces of constant velocity. It is therefore reasonable to study inviscid small amplitude unsteady perturbations of these flows.

Unfortunately the development in I is rather intricate and specific formulae are given only for the case of two-dimensional motion on a special class of parallel shear flows which are themselves a special case of the transversely sheared flows. Part of the purpose of the present paper is to generalize the results of I and to do so by a procedure that is much less complicated and considerably more straightforward. The new approach also provides some additional insight into the nature of the gust solutions on transversely sheared mean flows. More important, however, is the fact that the final formulae given in this paper are somewhat simpler than those given in I.

Another purpose of this paper is to extend the leading-edge scattering problem that was worked out in I for two-dimensional low frequency disturbances on a symmetric shear layer to three-dimensional disturbances on arbitrary shear layers.

The solutions are used to calculate the sound field that results from the scattering

of a gust by the edge of a plate. The formulae for the directivity patterns in the plane perpendicular to the plate, which reduce to the Ffowcs Williams & Hall (1970) formula in the limit of zero Mach number, constitute a generalization of that result which accounts for the effects of the surrounding mean flow field (fluid shielding, refraction, etc.). It is now recognized that such effects must be incorporated into Lighthill's (1952) theory to obtain accurate predictions of jet-noise directivity patterns for individual frequency bands and it turns out that this is also the case for edge noise, though the mean-flow effects are admittedly less severe here. It is shown that the results accurately predict the experimental third octave directivity patterns produced by a long flat plate in the mixing layer of a subsonic jet.

In STOL-aircraft applications, it is usually the trailing edge that is exposed to the intense turbulence. We therefore also calculate the sound field due to the scattering of a gust by a trailing edge. Since there is a mean flow in the vicinity of the plate, there is no difficulty in imposing a Kutta condition at the edge. The limit of zero Mach number is, of course, the same in this case as it is for a leading edge. But the mean-flow interaction effects are considerably different in these two cases. Thus in the low frequency limit the pressure-field radiation pattern (in the plane perpendicular to the plate) is given by the Ffowcs Williams & Hall (1970) result multiplied by two inverse Doppler factors for a leading edge and by only one inverse Doppler factor for a trailing edge. In both cases one Doppler factor is due to the convective motion of the gust relative to the stationary fluid at infinity, an effect that will occur even in the zero-mean-flow theories when the motion of the incident disturbance is properly accounted for. The additional Doppler factor in the leading-edge formula is due to mean-flow interaction effects. This is reminiscent of the remarkable low frequency lifting of the directivity pattern that is now well established for pure jet mixing noise (Goldstein 1975; Dowling, Ffowcs Williams & Goldstein 1978; Mani 1976). It is a rather surprising result of the present analysis that the low frequency lifting does not occur for a trailing edge.

In the high frequency limit the leading-edge directivity pattern (in the plane perpendicular to the plate) is very close to the Ffowcs Williams & Hall (1970) result, especially at points outside the zone of silence. Thus, as one might expect, the mean flow 'shields' the gust from the stationary fluid at infinity and thereby eliminates the convective amplification due to the relative motion of the incident disturbance and this stationary fluid.

On the other hand the mean flow alters the trailing-edge radiation pattern in a very unexpected way. Thus, when the Mach number is sufficiently high, it causes this pattern to be nearly the same as that due to a semi-infinite plate in the absence of a mean flow but with the plate extending to infinity in the downstream direction rather than in the upstream direction, i.e. it causes the leading and trailing edges to have the same directivity patterns when measured relative to the flow direction (rather than relative to the plate configuration as would be the case in the absence of a mean flow).

Finally it is shown how the gust solution can be used to explain qualitatively certain puzzling aspects of the behaviour of free shear flow turbulent convection velocities.

Rather than using the generalized-function approach of I we construct the gust solution in this paper by using the remarkable fact that the velocity and pressure fluctuations can be expressed in terms of two potentials, one of which is a purely

convected but otherwise arbitrary quantity that can be specified as a boundary condition and the other of which satisfies an inhomogeneous wave equation whose source term is a convected quantity which can also be specified as a boundary condition. This representation is deduced in § 2.1.

In § 2.2 we derive a formal solution to the wave equation that remains finite at all points of space. The flow field corresponds to the one that would exist if there are no 'scattering' surfaces or sources within the flow. It is then shown (in § 2.3) that the resulting expressions for the velocity and pressure fields closely resemble those of the gust solutions constructed in I and that they are in fact identical to them in the limiting case of two-dimensional motion treated in that paper. Consequently the solution constructed here is a generalization of the gust solution constructed in I.

Since the motion is now three-dimensional, the gust solution involves two arbitrary convected quantities rather than the single quantity that enters the solution in I. In fact, it can be shown that the most general 'everywhere finite' vortical convected solution on a *uniform* flow can also be expressed in terms of precisely two arbitrary convected quantities. But unlike that case, the velocity component in the direction of the mean velocity gradient now undergoes an algebraic decay at upstream infinity. The pressure fluctuations also undergo such a decay.

On the other hand the longitudinal velocity and remaining transverse velocity components need not decay at upstream infinity (as they would if the motion were two-dimensional) but rather behave like convected disturbances in this region. These two velocity components also differ from the pressure fluctuation and gradientwise velocity component in that they are 'driven' by both of the arbitrary convected quantities that enter the governing equations while the pressure and corresponding transverse velocity fluctuations are 'driven' by only one of these convected quantities. The latter convected quantity is shown to be equal to one of the components of the curl of the vorticity fluctuation far upstream in the flow. The other convected quantity is determined by the upstream value of either (but not both) of the fluctuating velocity components that it affects.

It is especially important that the gust solution is defined at all points of space and corresponds to the flow that would exist without any 'scattering' at other interacting surfaces in the flow. Thus it is normally possible to formulate a 'scattering' or distortion problem by assuming that the incident disturbance is specified far upstream in the flow where the 'scattered' solution has decayed. But in the present case the incident disturbance field must be represented by the gust solution whose transverse velocity component in the direction of the mean-flow velocity gradient will itself decay far upstream in the flow (in fact, when the motion is two-dimensional, the entire gust velocity field will decay in this region). We cannot therefore suppose that this velocity component is specified at upstream infinity† (i.e. at best we can incompletely specify the upstream velocity field). However, we can also formulate a 'scattering' problem that involves only experimentally observable inputs and outputs by requiring that the incident disturbance field be that which would be measured

† One of the referees has pointed out that this phenomenon is related to the algebraic growth in the downwind direction that certain modes of the unsteady motions are known to undergo. Naturally any mode that grows algebraically with axial distance cannot be defined at upstream infinity. This curious behaviour was examined to some extent by Durbin (1979) and Moffatt (1965).

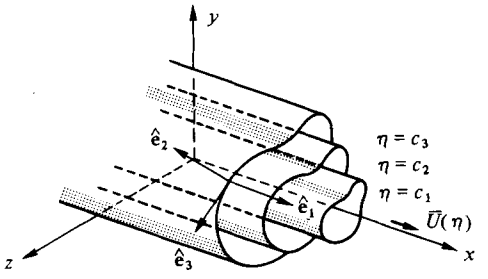

FIGURE 1. Cylindrical co-ordinate surfaces for transversely sheared flow.

with the scattering surfaces removed from the flow under consideration. We can then suppose that these surfaces are inserted into the flow and the combined 'scattered' and incident disturbance field is measured. This formulation will frequently correspond to the type of question we are most likely to ask in practice. The solution to the problem posed above is given by the gust solution plus the outgoing-wave solution that must be added to make the sum satisfy the boundary conditions on the scattering surfaces.

In § 3 we work out the solutions to the various scattering problems described above and show that the acoustic field is completely determined by a single component of the curl of the fluctuating vorticity far upstream in the flow while in the plane perpendicular to the plate it is determined by a single component of the upstream vorticity vector.

Finally the low and high frequency asymptotic expansions of the acoustic solution are compared with experimental data in § 3.5.

2. The gust solution on a transversely sheared mean flow

One of the simplest solutions to the inviscid non-heat-conducting equations of motion is provided by a unidirectional transversely sheared mean flow wherein the velocity $\mathbf{v}$, the density ρ and the pressure p are given by

$$\mathbf{v} = \hat{\mathbf{e}}_1 \bar{U}(\eta(y,z)), \quad \rho = \rho_0 = \text{constant}, \quad p = \text{constant} \tag{2.1}$$

respectively, where (x,y,z) are Cartesian co-ordinates, $\hat{\mathbf{e}}_1$ is a unit vector in the x direction and the transverse co-ordinate $\eta(y,z)$ is an arbitrary function of the rectangular co-ordinates (y, z) in the cross-flow direction. The surfaces on which η, and as a consequence the velocity $\bar{U}$, remain constant can be thought of as co-ordinate surfaces in a cylindrical co-ordinate system such as the one depicted in figure 1. Changes in $\bar{U}$ occur only in the direction $\nabla\eta$ normal to these surfaces. Thus when

$$\eta = r \equiv (y^2+z^2)^{\frac{1}{2}} \tag{2.2}$$

the co-ordinate surfaces become circular cylinders and, as a result, $\eta = r$ becomes the radial co-ordinate in a standard cylindrical co-ordinate system with polar axis in the x direction. In this case the velocity profiles are purely radial. On the other hand, when

$$\eta = y \tag{2.3}$$

the co-ordinate surfaces become parallel planes and the corresponding flow a parallel shear flow.

Over the years a wide range of inviscid fluid phenomena has been analysed by treating the unsteady motion as a small perturbation about some type of transversely sheared mean flow. Perhaps the most prominent of these have been in the area of hydrodynamic stability, where much of the literature is concerned with parallel sheared mean flows. However, there are also many analyses concerned with duct acoustics and jet noise that treat axially symmetric mean flows.

The inviscid linearized momentum and continuity equations governing the velocity and pressure perturbations on a transversely sheared mean flow, which we denote by $\mathbf{u}$ and p respectively, can be written as

$$\rho_0\left(\frac{D\mathbf{u}}{Dt}+\hat{\mathbf{e}}_1\frac{\bar{U}'}{g}v\right)=-\nabla p \tag{2.4}$$

and

$$\frac{1}{\rho_0 c_0^2}\frac{Dp}{Dt}+\nabla.\mathbf{u}=0, \tag{2.5}$$

where c_0 is the (constant) speed of sound of the mean flow, the prime denotes differentiation with respect to η, t denotes the time,

$$D/Dt=\partial/\partial t+\bar{U}(\eta)\,\partial/\partial x \tag{2.6}$$

is the mean-flow convective derivative,

$$g=1/|\nabla\eta| \tag{2.7}$$

and, since $\hat{\mathbf{e}}_2\equiv g\nabla\eta$ is the unit normal to the co-ordinate surfaces $\eta=$ constant,

$$v\equiv\mathbf{u}.\hat{\mathbf{e}}_2 \tag{2.8}$$

is the perturbation velocity component in the direction perpendicular to these surfaces. It is worth noting that the geometric weighting factor g is equal to unity in both the transverse co-ordinate systems discussed above.

2.1. *Introduction of potentials*

It can be seen by inspection that the linearized momentum equation (2.4) will be identically satisfied for any function ϕ of x, y, z and t and any function

$$\theta=\theta(x/\bar{U}(\eta)-t,y,z)$$

if we put

$$\mathbf{u}=\nabla\frac{D^2\phi}{Dt^2}+\frac{\bar{U}'}{g}\left[\hat{\mathbf{e}}_3\times\nabla\frac{D\phi}{Dt}+\hat{\mathbf{e}}_2\times\nabla\theta-2\frac{\bar{U}'}{g}\hat{\mathbf{e}}_1\frac{\partial\phi}{\partial x}\right] \tag{2.9}$$

and

$$p/\rho_0=-D^3\phi/Dt^3, \tag{2.10}$$

where $\hat{\mathbf{e}}_3=\hat{\mathbf{e}}_1\times\hat{\mathbf{e}}_2$ is the unit vector that forms a right-handed system with $\hat{\mathbf{e}}_1$ and $\hat{\mathbf{e}}_2$ as indicated in figure 1. This is rather easy to do for the parallel shear flow (2.3) and the reader who is interested in only this type of flow can set $g=1$ and $\eta=y$, recognize that $\hat{\mathbf{e}}_1$, $\hat{\mathbf{e}}_2$ and $\hat{\mathbf{e}}_3$ are the usual fixed unit vectors $\hat{\mathbf{i}}$, $\hat{\mathbf{j}}$ and $\hat{\mathbf{k}}$ in the x, y and z Cartesian co-ordinate directions and use the relation

$$\nabla=\hat{\mathbf{i}}\,\partial/\partial x+\hat{\mathbf{j}}\,\partial/\partial y+\hat{\mathbf{k}}\,\partial/\partial z$$

together with the fact that

$$D\theta/Dt=0. \tag{2.11}$$

But the reader who is interested in the general case must first introduce the family $\zeta(x, y) =$ constant of co-ordinate surfaces that are perpendicular to both the $\eta =$ constant and the $x =$ constant co-ordinate surfaces, recognize that η and ζ can be used as new independent variables in place of y and z, and then use the relations

$$\hat{\mathbf{e}}_3 = h\nabla\zeta, \quad h \equiv 1/|\nabla\zeta|, \tag{2.12}$$

$$\nabla = \hat{\mathbf{e}}_1 \frac{\partial}{\partial x} + \frac{\hat{\mathbf{e}}_2}{g}\frac{\partial}{\partial \eta} + \frac{\hat{\mathbf{e}}_3}{h}\frac{\partial}{\partial \zeta}, \tag{2.13}$$

where $\partial/\partial\eta$, of course, denotes the partial derivative with respect to η with x and ζ held fixed and similarly for $\partial/\partial\zeta$. Naturally (2.11) must also be used in this case.

Since the function ϕ is at this stage quite arbitrary it can be adjusted to ensure that the continuity equation (2.5) is also satisfied. Thus, substituting (2.9) and (2.10) into (2.5), we obtain after some manipulation (the reader who is interested in the general case must also use the usual formulae for the Laplacian and divergence in orthogonal curvilinear co-ordinates)

$$\frac{D}{Dt}\left[\left(\frac{1}{c_0^2}\frac{D^2}{Dt^2} - \nabla^2\right)\frac{D\phi}{Dt} - \frac{2}{hg}\frac{\partial^2}{\partial\eta\,\partial x}\left(\frac{\overline{U}'h}{g}\phi\right)\right] = 0$$

[where $g = h = 1$ and $\eta = y$ for the parallel shear flow (2.3)]. Notice that this equation does not involve the arbitrary function θ. It can be integrated immediately to obtain

$$\left(\frac{1}{c_0^2}\frac{D^2}{Dt^2} - \nabla^2\right)\frac{D\phi}{Dt} - \frac{2}{hg}\frac{\partial}{\partial\eta}\left(\frac{\overline{U}'h}{g}\frac{\partial\phi}{\partial x}\right) = -g\omega_c\left(\frac{x}{\overline{U}(\eta)} - t, y, z\right)\Big/\overline{U}', \tag{2.14}$$

where ω_c can be any function of its arguments.†

The factor $-g/\overline{U}'$, which has been inserted to simplify the subsequent equations, is equal to the reciprocal of the mean-flow vorticity. Then, since the left side of (2.14) is dimensionless, ω_c must have the dimensions of vorticity.

2.2. *Construction of gust solution*

We can in principle find a solution to the four scalar equations (2.4) and (2.5) that satisfies any appropriate boundary conditions by simply solving the wave equation (2.14) and substituting the result into (2.9) and (2.10). In fact, for any given set of boundary conditions, we can find at least one such solution for each choice of the arbitrary convected quantities θ and ω_c. In flows that persist for all time and extend infinitely far upstream these quantities are completely determined by the imposed upstream conditions. These statements become obvious when it is recognized that every solution to (2.4) can be expressed as the sum of (i) a particular solution that is defined and finite at all points of space and (ii) a homogeneous solution that satisfies a radiation condition at infinity‡ and causes the sum to satisfy the appropriate boundary conditions on any bounding surfaces that exist in the flow.

The part of the velocity and pressure fields generated by the particular solution and the term in (2.9) involving θ is defined over all space and represents (since our

† Flows with constant mean shear have very special properties. Möhring (1976) obtained a *second order* inhomogeneous wave equation for the axial velocity perturbation on this type of flow. However, his result cannot be generalized to more general shear flows and does not appear to be related to the one obtained here.

‡ For incompressible flow this can be replaced by a boundedness condition.

interest here is in 'external' flows that extend to infinity in all directions) the unsteady flow that would exist in the absence of any interacting boundary surfaces, i.e. it represents the part of the flow due to the imposed upstream conditions. Actually it only partially represents this portion of the flow since the wave equation (2.14) possesses homogeneous solutions corresponding to incident acoustic waves.

The part of the imposed upstream flow represented by the particular solution described above can be thought of as the hydrodynamic or non-acoustic part. We shall show subsequently that all the terms in this solution are proportional to one of the two arbitrary convected quantities θ and ω_c, so that the solution is in a sense 'driven' by these quantities.

Since our interest here is in motions that persist for all time (and not in the effects of initial transients or instabilities of the flow) we can without loss of generality restrict our attention to the case where the unsteady motion has harmonic time dependence. Then the convected quantities θ and ω_c become functions of the form

$$\omega_c = \Omega(y,z)\exp[i\omega(x/\overline{U}(\eta)-t)] \tag{2.15}$$

$$\theta = \Theta(y,z)\exp\{i\omega[x/\overline{U}(\eta)-t]\}, \tag{2.16}$$

where Ω and Θ are arbitrary functions of the cross-flow co-ordinates. The potential function ϕ can be written as

$$\phi = \overline{\phi}(x,y,z)\,e^{-i\omega t}. \tag{2.17}$$

Since the particular solution, which was described above, is defined over all space and since the coefficients of the wave equation (2.14) are independent of x, it is natural to attempt to construct this solution by taking the Fourier transform of (2.14) with respect to that variable. Then in view of (2.15)–(2.17), (2.14) becomes

$$\nabla_t^2[(\omega-\overline{U}k_1)\,\Phi]-\frac{2k_1}{hg}\frac{\partial}{\partial\eta}\left(\frac{\overline{U}'h}{g}\,\Phi\right)+\left[\left(\frac{\omega-\overline{U}k_1}{c_0}\right)^2-k_1^2\right](\omega-\overline{U}k_1)\,\Phi = \frac{ig\Omega(y,z)}{\overline{U}'}\,\delta\left(k_1-\frac{\omega}{\overline{U}}\right), \tag{2.18}$$

where

$$\Phi(k_1|y,z) \equiv \frac{1}{2\pi}\int_{-\infty}^{\infty}\exp(-ik_1x)\,\overline{\phi}\,(x,y,z)\,dx \tag{2.19}$$

is the Fourier transform of $\overline{\phi}$ and the transverse Laplacian ∇_t^2 is

$$\nabla_t^2 \equiv \frac{\partial^2}{\partial y^2}+\frac{\partial^2}{\partial z^2} = \frac{1}{hg}\left[\frac{\partial}{\partial\eta}\left(\frac{h}{g}\frac{\partial}{\partial\eta}\right)+\frac{\partial}{\partial\zeta}\left(\frac{g}{h}\frac{\partial}{\partial\zeta}\right)\right]. \tag{2.20}$$

In the general case of an arbitrary transversely sheared mean flow we can easily express the desired particular solution to (2.14) in terms of the free-space Green's function of the two-dimensional reduced wave operator on the left side of (2.18). But there is little to be gained by such generality and we now restrict our attention to a mean flow for which (2.18) can be solved by separation of variables. It turns out that the only flows for which this can be done are those corresponding to (2.2) and (2.3). Since parallel sheared flow is the simplest of these and since it was the one treated in I we consider only this case.

Then since $\zeta = z$ and $g = h = 1$ the coefficients of (2.18) will depend only on $\eta = y$ and we can suppose without loss of generality that

$$\Omega(y, z) = \bar{\Omega}(y|k_3) \exp(ik_3 z) \tag{2.21}$$

and

$$\Phi = \bar{\Phi}(k_1, y|k_3) \exp(ik_3 z), \tag{2.22}$$

so that (2.18) becomes

$$\Gamma'' - \left[\frac{2\bar{U}'k_1}{\omega - \bar{U}k_1}\Gamma\right]' + \left[\left(\frac{\omega - \bar{U}k_1}{c_0}\right)^2 - k_1^2 - k_3^2\right]\Gamma = -\frac{1}{i}\frac{\bar{\Omega}(y|k_3)}{\bar{U}'}\delta\left(k_1 - \frac{\omega}{\bar{U}}\right), \tag{2.23}$$

where

$$\Gamma \equiv (\omega - \bar{U}k_1)\bar{\Phi}. \tag{2.24}$$

Suppose that $\bar{U}' \to 0$ as $y \to \pm\infty$. Then in these regions the left side of (2.23) will approach the usual reduced wave equation for a uniformly moving medium. Consequently, (2.23) will possess two homogeneous solutions one of which, say Γ_U, satisfies a radiation condition at $y = +\infty$ and the other of which, say Γ_L, satisfies this condition at $y = -\infty$. The particular solution of (2.23) that is finite at *all* points of space and satisfies radiation conditions at $y = \pm\infty$ can therefore be written as

$$\begin{aligned}\Gamma = i\int_{-\infty}^{y} \bar{\Omega}(\eta)\frac{\Gamma_U(k_1, y)\,\Gamma_L(k_1, \eta)}{\bar{U}'(\eta)\,W(k_1, \eta)}\delta\left(k_1 - \frac{\omega}{\bar{U}(\eta)}\right)d\eta \\ + i\int_{y}^{\infty} \bar{\Omega}(\eta)\frac{\Gamma_L(k_1, y)\,\Gamma_U(k_1, \eta)}{\bar{U}'(\eta)\,W(k_1, \eta)}\delta\left(k_1 - \frac{\omega}{\bar{U}(\eta)}\right)d\eta,\end{aligned} \tag{2.25}$$

where for convenience we have suppressed the k_3 dependence of the various terms in this equation and

$$W(k_1, \eta) \equiv \Gamma_L(k_1, \eta)\,\Gamma_U'(k_1, \eta) - \Gamma_U(k_1, \eta)\,\Gamma_L'(k_1, \eta) \tag{2.26}$$

denotes the Wronskian of Γ_U and Γ_L.

Since $k_1 = \omega/\bar{U}$ is a singular point of (2.23) the individual factors in the integrand of (2.25) can become infinite at the point where the delta function becomes infinite, though they are grouped in a combination that will itself remain finite. In order to avoid this inconvenient ratio of infinite terms we notice that taking the Fourier transform of (2.10) and the y component of (2.4) yields

$$\Gamma = iP/\rho_0(\omega - \bar{U}k_1)^2, \quad V = P'/i\rho_0(\omega - \bar{U}k_1), \tag{2.27), (2.28}$$

where V and P are related to the transverse velocity and pressure fluctuations by

$$P \equiv \frac{1}{2\pi}\int_{-\infty}^{\infty} \exp[-i(k_1 x + k_3 z)]\,\bar{p}\,dx, \tag{2.29}$$

$$V = \frac{1}{2\pi}\int_{-\infty}^{\infty} \exp[-i(k_1 x + k_3 z)]\,\bar{v}\,dx \tag{2.30}$$

and

$$p = \bar{p}e^{-i\omega t}, \quad v = \bar{v}e^{-i\omega t}. \tag{2.31), (2.32}$$

Then since

$$(\omega - \bar{U}k_1)^2 W = -\frac{P_L P_U' - P_U P_L'}{\rho_0^2(\omega - \bar{U}k_1)} = \frac{P_L V_U - P_U V_L}{i(\omega - \bar{U}k_1)\rho_0} \tag{2.33}$$

[where (P_U, V_U) and (P_L, V_L) correspond to the solutions $\bar{\Phi}_U$ and $\bar{\Phi}_L$ in the manner dictated by (2.9) and (2.10)] and since P_U, P_L, V_U and V_L can all be expressed as linear combinations of the solutions† P_1, P_2, V_1 and V_2 whose behaviour is described by (3.4) and (3.5) of I, it follows from (2.27) and (2.33) that (2.25) can be written as

$$\Gamma = -\int_{-\infty}^{y} \bar{\Omega}(\eta)\,\frac{\Gamma_U(k_1,y)\,P_L(k_1,\eta)}{J(\eta)}\,\delta\left(k_1-\frac{\omega}{\bar{U}(\eta)}\right)d\eta$$
$$-\int_{y}^{\infty} \bar{\Omega}(\eta)\,\frac{\Gamma_L(k_1,y)\,P_U(k_1,\eta)}{J(\eta)}\,\delta\left(k_1-\frac{\omega}{\bar{U}(\eta)}\right)d\eta, \tag{2.34}$$

where

$$J(\eta) \equiv \bar{U}'(\eta)\lim_{k_1\to\omega/\bar{U}(\eta)}\frac{P_L(k_1,\eta)\,V_U(k_1,\eta)-P_U(k_1,\eta)\,V_L(k_1,\eta)}{i(\omega-\bar{U}k_1)} \tag{2.35}$$

exists and is non-zero and P_U and P_L remain finite at $k_1 = \omega/\bar{U}$.

The individual factors in the integrand of this equation are now well behaved and we can carry out the integration over the delta function. Thus inserting (2.34) into (2.24) and then inserting the result via (2.22) into the inverse of the transform (2.19), we obtain after integrating over the delta function

$$\bar{\phi} = -\exp(ik_3 z)\left[\int_{-\infty}^{y}\exp[i\omega x/\bar{U}(\eta)]\,\bar{\Omega}(\eta)\,\frac{\bar{\Phi}_U(\omega/\bar{U}(\eta),y)\,P_L(\omega/\bar{U}(\eta),\eta)}{J(\eta)}\,d\eta\right.$$
$$\left.+\int_{y}^{\infty}\exp[i\omega x/\bar{U}(\eta)]\,\bar{\Omega}(\eta)\,\frac{\bar{\Phi}_L(\omega/\bar{U}(\eta),y)\,P_U(\omega/\bar{U}(\eta),\eta)}{J(\eta)}\,d\eta\right], \tag{2.36}$$

where the k_3 dependence of the various terms in the integrand of this equation is still suppressed.

2.3. *Discussion of gust solution*

Inserting (2.36) into (2.17) and using the result in (2.9) and (2.10) (with $y = \eta$, $\zeta = z$ and $y = h = 1$), we obtain expressions for the velocity and pressure fluctuations of the gust. For example v_g, the y component of the gust velocity, becomes

$$v_g = \bar{v}_g e^{-i\omega t}, \tag{2.37}$$

where

$$\bar{v}_g = \exp(ik_3 z)\int_{-\infty}^{\infty}\exp[i\omega x/\bar{U}(\eta)]\,\bar{\Omega}(\eta)\,\mathscr{K}_v(y|\eta)\,d\eta \tag{2.38}$$

$$\mathscr{K}_v(y|\eta) = \begin{cases} -V_L(\omega/\bar{U}(\eta),y)\,P_U(\omega/\bar{U}(\eta),\eta)/J(\eta) & \text{for } \eta > y, \quad (2.39\,a)\\ -V_U(\omega/\bar{U}(\eta),y)\,P_L(\omega/\bar{U}(\eta),\eta)/J(\eta) & \text{for } \eta < y. \quad (2.39\,b)\end{cases}$$

Similar expressions can be obtained for the other gust-solution variables p_g, u_g and w_g. The only difference is that the V's on the right side of (2.39) must be replaced by the appropriate reduced variables (P in the case of p_g, etc.) and the contribution of the convected components (i.e. the terms involving θ) must be included for u_g and w_g.

These results closely resemble the formulae given in I. In fact it is shown in appendix A that (2.38) can be transformed into the corresponding transverse velocity component of equation (3.27) of I when the motion is two-dimensional (so that $k_3 = 0$)

† (P_1, V_1) and (P_2, V_2) denote corresponding solution pairs of the system of ordinary differentia equations governing the velocity and pressure fluctuations. The former are regular and the latter irregular at the regular singular point of these equations, which occurs at $\bar{U} = \omega/k_1$.

and that the procedure can easily be extended to obtain the other components of this equation. (In fact, since the transformations of appendix A do not require that $\bar{U}(-\infty) = \bar{U}(+\infty)$ or that the mean velocity profile has a single maximum or minimum, we have shown that equation (3.27) of I is actually more general than the assumptions used to derive it.)

The representation of the gust used in this paper differs from that given in I only because different sets of linearly independent solutions of the ordinary differential equations (i.e. P_U and P_L as opposed to P_1 and P_0) are used in equation (2.38) of this paper and equation (3.27) of I. The interpretative remarks given in § 3.3 of I therefore apply equally well to the results of the present paper but the new formulae are somewhat simpler than those given in I. Also, since they now arise as the particular solution of the inhomogeneous wave equation (2.14), the interpretation of the convected quantity

$$\omega_c(x/\bar{U}(y)-t, y, z) = \bar{\Omega}(y|k_3)\exp\{i[\omega(x/\bar{U}(y)-t)+k_3 z]\} \tag{2.40}$$

as a source that 'drives' the rest of the motion is now quite obvious.

Of course, (2.9) shows that there are two convected quantities (θ as well as ω_c) that 'drive' the flow when the unsteady motion is three-dimensional. But θ will have no effect on either the pressure fluctuations or the gradientwise velocity component while it drives the longitudinal and w components of the velocity in a very simple fashion. For example, it follows from (2.36) and (2.9) (with $y = \eta$ and $g = h = 1$) that the longitudinal gust velocity u_g is given by

$$u_g = \bar{u}_g e^{-i\omega t}, \tag{2.41}$$

$$\bar{u}_g = \exp(ik_3 z)\left[ik_3 \bar{U}'(y)\bar{\Theta}(y|k_3)\exp[i\omega x/\bar{U}(y)] + \int_{-\infty}^{\infty} \exp[i\omega x/\bar{U}(\eta)]\,\bar{\Omega}(\eta)\,\mathscr{K}_u(y|\eta)\,d\eta\right], \tag{2.42}$$

where

$$\theta(x/\bar{U}-t, y, z) = \bar{\Theta}(y|k_3)\exp\{i[\omega(x/\bar{U}(y)-t)+k_3 z]\} \tag{2.43}$$

and $\mathscr{K}_u$ is defined analogously to $\mathscr{K}_v$. Thus the axial velocity consists of a portion that is convected downstream at the local mean flow velocity plus a portion that consists of a superposition of disturbances travelling at all convection speeds between the maximum and minimum mean-flow velocities. But, when $\bar{\Omega}(y)$ is sharply peaked about some point y_0 in the flow, this second portion of u_g and the entire transverse disturbance v_g will both have convection velocities that remain nearly constant (i.e. independent of y) and take on values close to the mean velocity at y_0. This situation tends to occur in turbulent shear layers because the turbulent energy and consequently the turbulent vorticity of such flows are concentrated in a rather narrow region near the centre of the mixing layer where $\bar{U}'' \simeq 0$ and, as shown in § 5 of I or by the remarks given below [see (2.45)], ω_c is therefore nearly equal to the vorticity in low speed flows.

These results imply that the radial velocity correlations in the turbulent mixing layer of a round jet should have convection velocities that are more nearly constant across the mixing layer than the convection velocities of the longitudinal velocity correlations, the latter being more nearly equal to the local mean flow velocity. As can be seen from figure 2, the measurements taken by Wills (1964) in the mixing layer of a jet, two diameters downstream from the nozzle exit, show that this effect, though it is not strong, does indeed occur in practice.

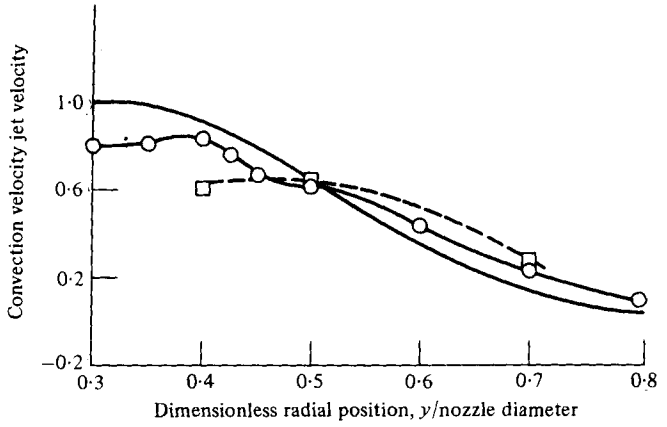

FIGURE 2. Variation of convection velocity across shear layer two diameters downstream from nozzle exit. ——, mean velocity; —○—, longitudinal component of convection velocity; —□—, radial component of convection velocity.

When the mean flow is uniform, all components of the gust velocity field are convected downstream at the mean flow speed. This is consistent with Taylor's hypothesis, which states that the turbulence will be nearly 'frozen' in a reference frame that moves with the mean flow. This gust solution is the most general motion on a uniform flow that is consistent with this requirement and is therefore frequently used to represent the turbulence in such flows.

Now there are two reasons why Taylor's hypothesis will not hold in real turbulent shear flows. One of these is that the turbulent velocity fluctuations cannot be treated as inviscid linear disturbances of the mean flow. This difficulty is common to all turbulent flows, in certain of which the turbulence is very close to being frozen. This occurs because the nonlinear and viscous effects require fairly large streamwise distances to produce significant deviations from Taylor's hypothesis in turbulent shear flows.

The other reason for the invalidity of Taylor's hypothesis is that the gust velocity field is no longer a purely convected quantity when the mean flow is non-uniform. As we have seen, the gusts in these flows contain components that travel at all speeds between the maximum and minimum flow velocities. However, we can introduce a generalized Taylor's hypothesis for shear flows by supposing that the turbulence can be represented by the gust solution deduced above (which, as we have seen, is a generalization of the uniform-flow gust solution). The convection properties of the turbulence will then be those implied by this representation rather than those of Taylor's hypothesis.

As we have indicated, this representation of the turbulence will not apply over streamwise distances that are long enough to allow viscous and nonlinear effects (including the effects of the slow divergence of the shear layer) to take place. But we can calculate the turbulence over distances that are small compared with the ratio of the mean to the turbulent velocity times the integral scale of the turbulence by linearizing the unsteady motion about its value at some fixed streamwise location (Hunt 1977). The gust solution will then represent the turbulence in this local sense.

Now, unlike the case where the mean flow is uniform, the equations for a transversely sheared mean flow possess harmonic instability-wave solutions that grow

exponentially fast in the streamwise direction and these solutions have been used to explain certain features of real turbulent flows. But at any given frequency and transverse wavenumber (in the η direction), the class of unsteady motions that can be represented as a superposition of instability waves is much more restricted than that which can be represented by the most general gust solution. This is because there is only a relatively small number of instability waves (usually one) at any given frequency and η-direction wavenumber while the gust is an arbitrary superposition of a non-denumerably infinite number of waves (i.e. it has a continuous spectrum). Thus the instability waves cannot by themselves represent the complete turbulence velocity field at any given streamwise location. The only question is whether or not they must be added to the gust solution in order to obtain a complete local representation of the turbulence. In this regard it can be argued that the instability waves model those features of the turbulence that are associated with the maintenance of the turbulent energy and are therefore related to the relatively slow growth of the turbulent eddies as they are convected downstream. Since such processes take place over axial distances that are much larger than the length over which the local linearization representation is valid, it is quite possible that the instability waves will play no role in this representation and can therefore be excluded by requiring that the solution should remain finite at all points of space.

The particle displacement λ in the direction transverse to the surfaces of constant mean velocity (see figure 1) is defined in terms of the velocity v in that direction by $v = D\lambda/Dt$. But it follows from (2.13) and the η component of (2.9) that this quantity differs from the quantity λ defined in (B1) by only an arbitrary additive convected quantity. We can make the definition of the particle displacement unique by setting this quantity to zero. Then (B 2) and (B 3) show that the two convected quantities ω_c and θ that 'drive' the gust solution are linearly related to the ζ and x components of the vorticity (ω_ζ and ω_x respectively), the pressure fluctuations and the particle displacement in the manner indicated by (B 2). In the absence of the gust solution the right side of (B 2) must vanish and in the general case, since it is easy to see that the left side of this equation is itself a convected quantity, the convective derivative D/Dt of the right side must vanish.

For a parallel shear flow (where $y = \eta$, $\zeta = z$ and $g = h = 1$) γ is zero and (B 2) becomes

$$\frac{\partial \omega_c}{\partial x} = \frac{\partial}{\partial x}\left[\omega_z + \overline{U}' \frac{p}{\rho_0 c_0^2} - \overline{U}''\lambda\right] - \frac{\partial \omega_x}{\partial z}. \tag{2.44}$$

Thus in this case we can express the convected quantity ω_c directly in terms of the somewhat more physical quantities that appear on the right of the equation. In fact, since the procedure near the end of § 3.2 of I can be used to show that λ and p (as well as all the terms in (2.9) that involve ϕ) will always decay algebraically as $x \to -\infty$, it follows that

$$\frac{\partial \omega_c}{\partial x} \to \left(\frac{\partial \omega_z}{\partial x} - \frac{\partial \omega_x}{\partial z}\right) \quad \text{as} \quad x \to -\infty. \tag{2.45}$$

Consequently (2.15) implies that

$$\Omega(y,z)\exp\left[i\omega(x/\overline{U} - t)\right] \to \frac{\overline{U}}{i\omega}\left(\frac{\partial \omega_z}{\partial x} - \frac{\partial \omega_x}{\partial z}\right) \quad \text{as} \quad x \to -\infty$$

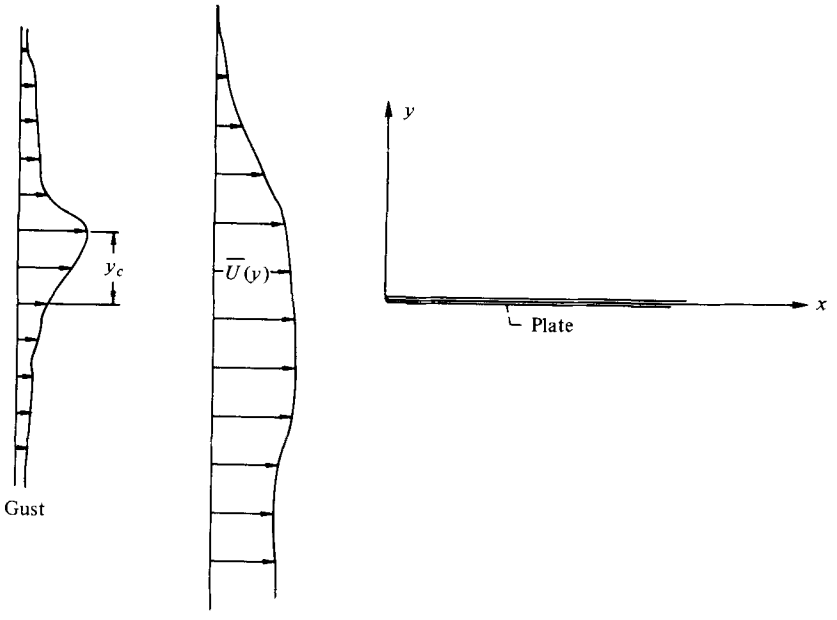

FIGURE 3. Geometry for leading-edge scattering problem.

when the motion has harmonic time dependence. Then the amplitude $\bar{\Omega}$ in (2.40) is related to the upstream vorticity by

$$\bar{\Omega}(y|k_3) = \frac{\bar{U}}{i\omega} \lim_{x\to-\infty} \frac{\exp[i\omega(t-x/\bar{U})]}{2\pi} \int_{-\infty}^{\infty} \left(\frac{\partial\omega_z}{\partial x} - \frac{\partial\omega_x}{\partial z}\right) \exp(-ik_3 z)\, dz. \quad (2.46)$$

When the motion has arbitrary time dependence $\bar{\Omega}$ is related to the upstream vorticity by

$$\bar{\Omega}(y|k_3) = \frac{\bar{U}}{i\omega} \lim_{x\to-\infty} \frac{1}{(2\pi)^2} \int_{-\infty}^{\infty}\int_{-\infty}^{\infty} \exp\{i[\omega(t-x/\bar{U}) - k_3 z]\} \times \left(\frac{\partial\omega_z}{\partial x} - \frac{\partial\omega_x}{\partial z}\right) dz\, dt. \quad (2.47)$$

It therefore follows from (2.10), (2.36) and (2.38) that *the potential ϕ as well as the pressure p and the y component of the velocity v are completely determined by the upstream distribution of the quantity $\hat{\mathbf{e}}_2 . \nabla \times \boldsymbol{\omega}$, i.e. the y component of the curl of the vorticity vector.*

On the other hand, the longitudinal and z components of the velocity, u and w, respectively, depend on θ as well as on ϕ and are therefore only incompletely determined by the upstream value of $\hat{\mathbf{e}}_2 . \nabla \times \boldsymbol{\omega}$. But since all terms of (2.9) that involve ϕ must decay as $x \to -\infty$, it follows that

$$\left.\begin{aligned} u_g &\to \bar{U}' \frac{\partial}{\partial z}\theta\left(\frac{x}{\bar{U}} - t, y, z\right) \\ w_g &\to -\bar{U}' \frac{\partial}{\partial x}\theta\left(\frac{x}{\bar{U}} - t, y, z\right) \end{aligned}\right\} \quad \text{as} \quad x \to -\infty,$$

so that *u_g and w_g behave like convected disturbances at upstream infinity and the specification of one (but not both) of these disturbances along with the y component of $\nabla \times \boldsymbol{\omega}$ will uniquely determine the gust solution at all points of the flow.*

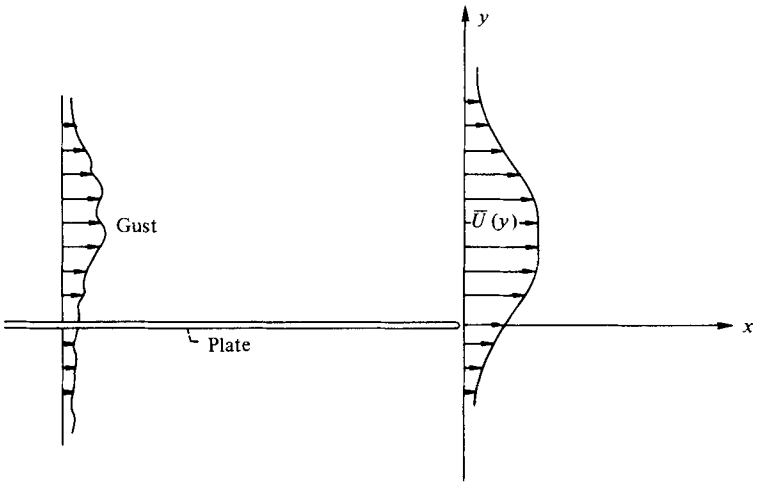

FIGURE 4. Geometry for trailing-edge scattering problem.

Equation (2.44) is a generalization of a result obtained by Möhring (1976) and Durbin (1979) for a flow with *constant mean shear* (i.e. with $\bar{U}'' \equiv 0$). When the motion is two-dimensional ω_x is zero and (2.44) reduces to $\omega_c = \omega_z + \bar{U}'(p/\rho_0 c_0^2) - \bar{U}''\lambda$, which, except for differences in notation, is the same as equation (5.3) of I. Then, as in I, $\omega_c \to \omega_z$ as $x \to -\infty$ and $\theta \equiv 0$ at all points of the flow. In this case ω_c represents the unsteady upstream vorticity and the source term on the right side of (2.14) is the ratio of this unsteady vorticity to the vorticity of the mean flow.

3. Interaction of a gust with a half-plane

In I we calculated the acoustic field that is produced when a two-dimensional symmetric gust on a symmetric shear layer interacts with a semi-infinite plate that extends infinitely far downstream. Explicit formulae were given only for the limiting case where the gust wavelength was large compared with the transverse dimensions of the shear layer. In this section we shall generalize that solution in a number of ways. We first consider, as we did in I, the scattering of a harmonic gust by a semi-infinite plate that extends to downstream infinity in a two-dimensional shear layer (see figure 3). But we now allow the gust to be an arbitrary (in general asymmetric) three-dimensional disturbance and let the mean velocity distribution be an arbitrary function of y. Moreover we now obtain explicit formulae for the case where the wavelength of the gust is small compared with the transverse dimensions of the shear layer as well as for the case where it is large. Finally, it is shown how this 'leading-edge' solution can be modified so that it applies to the trailing-edge scattering problem depicted in figure 4.

For both of these configurations the solution to the problem is equal to the sum of the gust solution whose transverse velocity field is given by (2.38) and a 'scattered' part, say $\{\bar{p}_a e^{-i\omega t}, \bar{u}_a e^{-i\omega t}, \bar{v}_a e^{-i\omega t}, \bar{w}_a e^{-i\omega t}\}$, which has outgoing-wave behaviour at infinity (i.e. it satisfies a radiation condition) and has an upwash velocity component (i.e. a y-velocity component) at the surface of the plate that is equal and opposite to the upwash (i.e. gradientwise) component $\bar{v}_g e^{-i\omega t}$ of the gust solution (2.38).

Since the flow extends to infinity in all directions, the pressure and upwash amplitude

of the 'scattered' solution can be expressed in terms of the outgoing-wave solutions P_U, V_U, P_L and V_L introduced in the previous section by

$$\bar{p}_a = \exp(ik_3 z)\int_{-\infty}^{\infty} \exp(ik_1 x)\, A_\sigma(k_1|k_3)\, P_\sigma(k_1, y|k_3)\, dk_1, \tag{3.1a}$$

$$\bar{v}_a = \exp(ik_3 z)\int_{-\infty}^{\infty} \exp(ik_1 x)\, A_\sigma(k_1|k_3)\, V_\sigma(k_1, y|k_3)\, dk_1, \tag{3.1b}$$

where $\sigma = U, L$ for $y \gtrless 0$. Since the continuity of $\bar{v}_g$ across the plane $y = 0$ implies that $\bar{v}_a$ must also exhibit this continuity (if the imposed upwash velocity is to be continuous across the portion of this plane not occupied by the plate and zero on the plate surface) the expansion coefficients A_U and A_L must be related by

$$A_U(k_1|k_3)\, V_U(k_1, 0|k_3) = A_L(k_1|k_3)\, V_L(k_1, 0|k_3). \tag{3.2}$$

As is usual in problems of this type, we suppose that ω has a small positive imaginary part that will be put equal to zero at the end of the analysis.

3.1. *The leading-edge scattering problem*

We first consider the case where the plate extends to infinity in the downstream direction. Then the configuration is the one illustrated in figure 3. The boundary conditions on the plane $y = 0$ are

$$\bar{v}_a(x, 0, z) = -\bar{v}_g(x, 0, z) \quad \text{for} \quad x > 0, \quad -\infty < z < \infty,$$

$$\bar{p}_a(x, 0+, z) = \bar{p}_a(x, 0-, z) \quad \text{for} \quad x < 0, \quad -\infty < z < \infty,$$

where $0\pm$ denote the limiting values as y approaches zero from above/below.

Inserting (3.1) and (3.2) into these relations, we find that $A_U(k_1|k_3)$ can be calculated by solving the following dual integral equations:

$$\int_{-\infty}^{\infty} \exp(ik_1 x)\, A_U(k_1)\left[P_U(k_1, 0) - V_U(k_1, 0)\frac{P_L(k_1, 0)}{V_L(k_1, 0)}\right] dk_1 = 0 \quad \text{for} \quad x < 0,$$

$$-\bar{v}_g \exp(-ik_3 z) = \int_{-\infty}^{\infty} \exp(ik_1 x)\, A_U(k_1)\, V_U(k_1, 0)\, dk_1 \quad \text{for} \quad x > 0,$$

where, as before, we have dropped the k_3 dependence from the notation and $\bar{v}_g$ is given by (2.38).

These equations can be solved for $A_U(k_1)$ by the Wiener–Hopf technique and the result can be substituted into (3.1*a*) to obtain an expression for the scattered portion of the pressure field. Since the procedure is nearly identical to the one used in § 6.1 of I we give only the final result, which can be written as

$$\bar{p}_a(x, y|k_3) = \exp(ik_3 z)\int_{-\infty}^{\infty} \bar{\Omega}(\eta|k_3)\, \mathscr{K}_v(0|\eta, k_3)\, R(x, y|\eta, k_3)\, d\eta, \tag{3.3}$$

where $\mathscr{K}_v$ is defined by (2.39), $\bar{\Omega}$ is related to the y component of the curl of the vorticity at upstream infinity by (2.47),

$$R(x, y|\eta, k_3) = \frac{\bar{U}(\eta)}{2\pi i}\int_{-\infty}^{\infty} \frac{\exp(ik_1 x)\, \kappa_+(\omega/\bar{U}(\eta)|k_3)\, P_\sigma(k_1, y|k_3)}{[\omega - k_1 \bar{U}(\eta)]\, \kappa_+(k_1|k_3)\, V_\sigma(k_1, 0|k_3)}\, dk_1,$$

$$\sigma = U, L \quad \text{for} \quad y \gtrless 0, \tag{3.4}$$

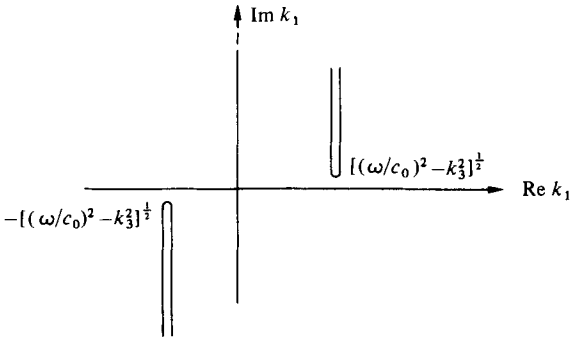

FIGURE 5. Branch cuts for square root in complex k_1 plane.

and $\kappa_\pm(k_1, k_3)$ denote non-zero analytic functions in the upper/lower half of the complex k_1 plane with algebraic behaviour at infinity. These functions are uniquely determined (to within an irrelevant multiplicative constant) by their behaviour along the real axis, which is given by

$$\frac{\kappa_+(k_1|k_3)}{\kappa_-(k_1|k_3)} = \frac{P_U(k_1, 0|k_3)}{\overline{V}_U(k_1, 0|k_3)} - \frac{P_L(k_1, 0|k_3)}{\overline{V}_L(k_1, 0|k_3)}. \tag{3.5}$$

The amplitude of the 'scattered' pressure field $\tilde{p}_a(x, y, z)\, e^{-i\omega t}$ due to a harmonic gust with a distribution of transverse wavenumbers k_3 can now be calculated simply by integrating (3.3) with respect to k_3 to obtain

$$\tilde{p}_a(x, y, z) = \int_{-\infty}^{\infty}\int_{-\infty}^{\infty} \exp(ik_3 z)\, \overline{\Omega}(\eta|k_3)\, \mathscr{K}_v(0|\eta, k_3)\, R(x, y|\eta, k_3)\, d\eta\, dk_3. \tag{3.6}$$

Since $\overline{p}_g$ is continuous across the plate, this result can be used to calculate the jump in pressure across the plate and consequently the net fluctuating force acting on any given length of the plate (i.e. the response function for that length of plate). We can also use it to calculate the acoustic pressure radiated by the plate, since $\overline{p}_g$ decays exponentially fast as $y \to \infty$ whenever the magnitude of the difference between the maximum Mach number in the shear layer and the Mach number at ∞ is less than unity (see p. 315 of I).

The pressure jump across the plate is calculated in appendix C. We shall discuss the calculation of the acoustic pressure fluctuations only for the case where the observation point is above the plate we shall suppose that $\overline{U}(y) \to 0$ as $y \to \infty$. Then

$$P_U \sim C_0(k_1|k_3)\, e^{-\gamma y} \quad \text{as} \quad y \to +\infty, \tag{3.7}$$

where $C_0(k_1|k_3)$ is a constant,

$$\gamma \equiv [k_1^2 - (\omega/c_0)^2 + k_3^2]^{\frac{1}{2}} \tag{3.8}$$

and the branch cut for the square root is the one indicated in figure 5.

Inserting this into (3.4), introducing the polar co-ordinates

$$x = R\sin\theta\cos\phi, \quad y = R\sin\theta\sin\phi, \quad z = R\cos\theta \tag{3.9}$$

depicted in figure 6 and using the method of stationary phase in the usual way to obtain the asymptotic expansions as $R \to \infty$ of the contour integrals with respect to k_1 and k_3 in (3.4) and (3.6) respectively, we obtain

$$\tilde{p}_a(R, \theta, \phi) \sim -\frac{\sin\theta\sin\phi}{R} \exp(ik_0 R) \int_{-\infty}^{\infty} \overline{\Omega}(\eta|k_0\cos\theta)\, \mathscr{K}_v(0|\eta, k_0\cos\theta) \times T(\eta, \theta, \theta_0)\, d\eta, \tag{3.10}$$

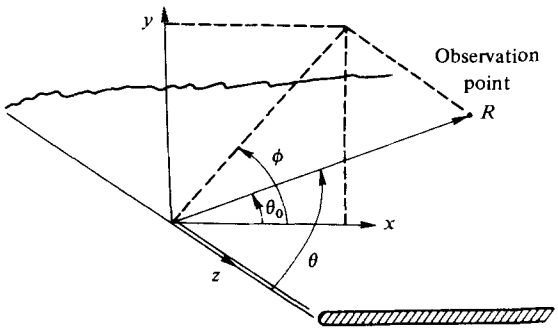

FIGURE 6. Polar co-ordinate system for radiation field.

where

$$T(\eta,\theta,\theta_0) = T_{le}(\eta,\theta,\theta_0)$$
$$\equiv \frac{M(\eta)\,C_0(k_0\cos\theta_0|k_0\cos\theta)\,\kappa_+(k_0/M(\eta)|k_0\cos\theta)}{[1-M(\eta)\cos\theta_0]\,\kappa_+(k_0\cos\theta_0|k_0\cos\theta)\,V_U(k_0\cos\theta_0,0|k_0\cos\theta)}, \tag{3.11}$$

we have put

$$M(\eta)\equiv \bar{U}(\eta)/c_0, \quad k_0\equiv \omega/c_0 \tag{3.12), (3.13}$$

and the angle θ_0 depicted in figure 6 is defined by

$$\cos\theta_0 \equiv \sin\theta\cos\phi. \tag{3.14}$$

Equations (2.47) and (3.10) show that the radiated sound produced by the gust depends *only* on the y component of the curl of its vorticity field far upstream of the leading edge of the plate. *No other property of the gust can affect the sound field or for that matter the pressure fluctuations at any point of the flow.*

In the plane perpendicular to the plate where $\theta = \frac{1}{2}\pi$ the acoustic field will depend only on $\bar{\Omega}(\eta|0)$. But since the second term on the right side of (2.47) will integrate to zero (provided that ω_x is sufficiently localized) when $k_3 = 0$, $\bar{\Omega}(\eta|0)$ and consequently the acoustic field itself will depend only on the upstream values of the z component of the incident vorticity field (as it does when the motion is two-dimensional). Moreover only the solutions of the ordinary differential equations for two-dimensional motion will enter the calculation of $\mathscr{K}_v$ and T. Finally it is worth noting that only a single transverse wavenumber component of the upstream vorticity curl can affect the sound field at any given value of θ.

3.2. *The trailing-edge scattering problem*

Now suppose that the plate extends to upstream infinity as shown in figure 4. The gust solution is the same as before but the boundary conditions for the 'scattered' solution now become

$$\bar{v}_a(x,0,z) = -\bar{v}_g(x,0,z) \quad \text{for} \quad x<0, \quad -\infty<z<\infty,$$

and

$$\bar{p}_a(x,0+,z) = \bar{p}_a(x,0-,z) \quad \text{for} \quad x>0, \quad -\infty<z<\infty.$$

We suppose that the mean flow $\bar{U}(0)$ is non-zero and continuous at $y = 0$, i.e. at the surface of the plate, though we can assume it to be as small as we like, and require that a Kutta condition be satisfied at the trailing edge.

The problem now amounts to solving the dual integral equations

$$\int_{-\infty}^{\infty} \exp(ik_1 x) A_U(k_1) \left[P_U(k_1, 0) - V_U(k_1, 0) \frac{P_L(k_1, 0)}{V_L(k_1, 0)} \right] dk_1 = 0 \quad \text{for} \quad x > 0,$$

$$-\bar{v}_y \exp(-ik_3 z) = \int_{-\infty}^{\infty} \exp(ik_1 x) A_U(k_1) V_U(k_1, 0)\, dk_1 \quad \text{for} \quad x < 0.$$

The procedure is nearly the same as before and we therefore give only the final results. The pressure jump across the plate is given in appendix C. The acoustic pressure fluctuations are still given by (3.10) but with T now given by

$$\begin{aligned} T(\eta, \theta, \theta_0) &= T_{te}(\eta, \theta, \theta_0) \\ &\equiv \frac{-M(\eta) C_0(k_0 \cos\theta_0 | k_0 \cos\theta)\, \kappa_-(k_0 \cos\theta_0 | k_0 \cos\theta)}{[1 - M(\eta)\cos\theta_0]\, \kappa_-(k_0/M(\eta) | k_0 \cos\theta)\, V_U(k_0 \cos\theta_0, 0 | k_0 \cos\theta)} \end{aligned} \tag{3.15}$$

rather than by (3.11).

In order to make these formulae explicit we must know the solutions to the ordinary differential equations governing the reduced variables P and V. These solutions must in most cases be determined numerically. But explicit simple asymptotic formulae can be obtained when the wavelength is either very large or very small compared with some characteristic dimensions δ of the shear layer.

3.3. *Low frequency solution*

We first consider the low frequency limit, where $k_0 \delta \ll 1$. In addition to requiring that $\bar{U}(y) \to 0$ as $y \to +\infty$, we also suppose for simplicity that $\bar{U}(y) \to 0$ as $y \to -\infty$. The solutions can be found by using the method of matched asymptotic expansions as was done for the two-dimensional case in § 6.3 of I. The procedure is almost identical and we again give only the final results. Thus when $y = O(\delta)$

$$P_U(k_1, y | k_3) = C_0(k_1 | k_3) + O(k_0 \delta), \tag{3.16}$$

$$V_U(k_1, y | k_3) = \frac{iC_0(k_1 | k_3)}{\rho_0 c_0 k_0^2} (k_1^2 + k_3^2 - k_0^2)^{\frac{1}{2}} [k_0 - k_1 M(y)] + O(k_0 \delta) \tag{3.17}$$

and

$$V_L / P_L = -V_U / P_U, \tag{3.18}$$

where $C_0(k_1 | k_3)$ is the constant defined by (3.7).

Inserting these results into (3.5), we find by inspection that

$$\kappa_+(k_1 | k_3) = [k_1 + (k_0^2 - k_3^2)^{\frac{1}{2}}]^{-\frac{1}{2}}, \tag{3.19}$$

and using this together with (3.16) and (3.17) in (3.10), (3.11) and (3.15), we find upon combining results that

$$\begin{aligned} \frac{\tilde{p}_a}{\rho_0 c_0} \sim -\frac{(\cos\tfrac{1}{2}\phi) \exp(ik_0 R)}{R[1 - M(0)\cos\theta_0]} \int_{-\infty}^{\infty} \left[\frac{2M(\eta)\sin\theta}{1 + M(\eta)\sin\theta} \right]^{\frac{1}{2}} \\ \times \frac{M(\eta)\, \bar{\Omega}(\eta | k_0 \cos\theta)\, \mathscr{K}_v(0 | \eta, k_0 \cos\theta)}{1 - M(\eta)\cos\theta_0}\, d\eta \end{aligned} \tag{3.20a}$$

for a leading edge and

$$\frac{\tilde{p}_a}{\rho_0 c_0} \sim -\frac{(\sin\tfrac{1}{2}\phi)\exp(ik_0 R)}{R}\int_{-\infty}^{\infty}\left[\frac{-2M(\eta)\sin\theta}{1-M(\eta)\sin\theta}\right]^{\frac{1}{2}} \times \frac{M(\eta)\,\bar{\Omega}(\eta|k_0\cos\theta)\,\mathscr{K}_v(0|\eta,k_0\cos\theta)}{[1-M(0)/M(\eta)][1-M(\eta)\cos\theta_0]}\,d\eta \tag{3.20b}$$

for a trailing edge.

Inserting (3.16) and (3.17) into (2.35) and (2.39), we find that $\mathscr{K}_v(0|\eta,k_0\cos\theta)$ is actually independent of θ and is given by

$$\mathscr{K}_v(0|\eta,k_0\cos\theta) = ik_0(\operatorname{sgn}\eta)\,[M(\eta)-M(0)]/2M'(\eta)\,M(\eta). \tag{3.21}$$

These results clearly show that the acoustic pressure field is the superposition of the elementary acoustic fields produced by the upstream vorticity $\bar{\Omega}(y|k_0\cos\theta)$ residing at each level y above/below the plate.

We have already indicated that the vorticity distribution tends to be sharply peaked in shear layers. When this occurs the terms multipying $\bar{\Omega}$ in the integrands of the above equations can be replaced by their values at the height y_c where $\bar{\Omega}$ is maximum. Then in the plane perpendicular to the plate where $\theta = \frac{1}{2}\pi$ and $\theta_0 = \phi$, the directivity patterns of the mean-square acoustic pressures will be given by

$$\frac{\cos^2\tfrac{1}{2}\phi}{[1-M(0)\cos\phi]^2[1-M(y_c)\cos\phi]^2} \quad \text{for a leading edge} \tag{3.22}$$

and

$$\frac{\sin^2\tfrac{1}{2}\phi}{[1-M(y_c)\cos\phi]^2} \quad \text{for a trailing edge.} \tag{3.23}$$

When $M = 0$ these results both reduce to the $\cos^2\frac{1}{2}\phi$ directivity pattern found by Ffowcs Williams & Hall (1970) for the scattering by an edge in the absence of a mean flow. The trailing-edge formula reduces to $\sin^2\frac{1}{2}\phi = \cos^2\frac{1}{2}(\pi-\phi)$ because the angle ϕ is measured relative to a line extending downstream from the plate in this case (since the polar co-ordinates are always oriented relative to the mean flow direction) rather than being measured relative to the plate itself as it is in both the Ffowcs Williams & Hall result and the leading edge directivity formula given above.

Thus in the low frequency limit the shear layer alters the directivity pattern by four inverse powers of the Doppler factor for a leading edge and by two inverse powers for a trailing edge. In both cases two of the inverse Doppler factors are due to the convective motion of the incident gust relative to the stationary fluid at infinity. The additional two inverse Doppler factors that appear in the leading-edge formula are due to a mean-flow interaction effect. This low frequency 'lifting' of the directivity pattern by the mean flow is already well established for pure jet mixing noise (Goldstein 1975, 1976; Dowling *et al.* 1978; Mani 1976). The remarkable fact is that this effect does not occur for a trailing edge.

3.4. *High frequency solution*

We now consider the high frequency limit, where $k_0\delta \gg 1$. In this case the solution can be found by the WKBJ method (Mörse & Feshbach 1953, pp. 1092–1105).

It follows from (2.23) and (2.27) that the homogeneous solutions P_U and P_L must satisfy

$$D^2(P'/D^2)' + k_0^2(D^2-\tilde{k}_1^2-\tilde{k}_3^2)\,P = 0, \tag{3.24}$$

where we have put

$$D \equiv 1 - \tilde{k}_1 M(y), \tag{3.25}$$

$$\tilde{k}_1 = k_1/k_0, \quad \tilde{k}_3 = k_3/k_0. \tag{3.26}$$

If all lengths in this equation are assumed to be non-dimensionalized by the thickness δ of the shear layer then k_0 will appear only in the combination $k_0\delta$, which we suppose to be large, while $\tilde{k}_1$ and $\tilde{k}_3$ are assumed to be of order unity. We now proceed in the usual way and reduce this equation to normal form by introducing the new dependent variable

$$\Pi = P/D \tag{3.27}$$

to obtain

$$\Pi'' + (k_0^2 q + s)\,\Pi = 0, \tag{3.28}$$

where

$$s = (D''/D) - 2(D'/D)^2 \tag{3.29}$$

and

$$q = D^2 - \tilde{k}_1^2 - \tilde{k}_3^2. \tag{3.30}$$

The turning points of this equation (i.e. the points where $q = 0$) are located where

$$M(y) = \pm[1 + (\tilde{k}_3/\tilde{k}_1)^2]^{\frac{1}{2}} + \tilde{k}_1^{-1}. \tag{3.31}$$

We shall suppose that the flow is subsonic and that the velocity profile is monotonic. Then since we are assuming that $M(y) > 0$, there will be at most one turning point, which will occur where

$$M(y) = -[1 + (k_3/k_1)^2]^{\frac{1}{2}} + \tilde{k}_1^{-1} \quad \text{when} \quad 0 < \tilde{k}_1 < 1 \tag{3.32}$$

and where

$$M(y) = [1 + (k_3/k_1)^2]^{\frac{1}{2}} + \tilde{k}_1^{-1} \quad \text{when} \quad \tilde{k}_1 < 0. \tag{3.33}$$

It can be seen from the formulae in § 3.2 that the terms in the far-field equations are all evaluated at $\tilde{k}_3 \equiv k_3/k_0 = \cos\theta$ and either at $\tilde{k}_1 \equiv k_1/k_0 = \cos\theta_0$ or at $\tilde{k}_1 = 1/M(\eta)$. There will be no turning point in the second case and when the observation point is in the plane perpendicular to the plate, so that $\theta = \frac{1}{2}\pi$, the turning point will be given by (3.32) in the first case.

When there are no turning points (3.28) possesses the two linearly independent asymptotic solutions (Mörse & Feshbach 1953, pp. 1092–1105)

$$\Pi_\pm \sim \exp\left(\pm ik_0 \int_0^y [q(y)]^{\frac{1}{2}}\,dy\right) \Big/ [q(y)]^{\frac{1}{4}} \quad \text{as} \quad k_0\delta \to \infty. \tag{3.34}$$

When there is a turning point, say y_δ, lying within the shear layer (3.28) possesses the two linearly independent asymptotic solutions

$$\Pi_+ \sim \left(\frac{k_0\pi}{3}\right)^{\frac{1}{2}} \frac{\zeta^{\frac{3}{4}}}{q^{\frac{1}{4}}}\, H_{\frac{1}{3}}^{(1)}(\tfrac{2}{3}k_0\zeta^{\frac{3}{2}})\, e^{\frac{5}{12}i\pi} \quad \text{as} \quad k_0\delta \to \infty$$

and

$$\Pi_- \sim \left(\frac{k_0\pi}{3}\right)^{\frac{1}{2}} \frac{\zeta^{\frac{3}{4}}}{q^{\frac{1}{4}}}\, H_{\frac{1}{3}}^{(2)}(\tfrac{2}{3}k_0\zeta^{\frac{3}{2}})\, e^{-\frac{5}{12}i\pi} \quad \text{as} \quad k_0\delta \to \infty,$$

where the H's denote Hankel functions and

$$\zeta \equiv \pm\left(\frac{3}{2}\int_{y_\delta}^{y} [\pm q(y)]^{\frac{1}{2}}\,dy\right)^{\frac{2}{3}} \quad \text{for} \quad y \gtrless y_\delta.$$

Then when y is not in the immediate vicinity of the turning point, $k_0\zeta$ will be large and we can replace the Hankel functions by their large argument asymptotic expansions to obtain (Abramowitz & Stegun 1964, p. 364)

$$\Pi_+ \sim \exp\left(ik_0\int_{y_\delta}^{y}[q(y)]^{\frac{1}{2}}\,dy\right)\Big/[q(y)]^{\frac{1}{4}} \quad \text{for} \quad y \neq y_\delta, \quad k_0\delta\to\infty, \tag{3.35}$$

$$\Pi_- \sim \begin{cases} \dfrac{2e^{\frac{1}{4}i\pi}\cos\left[k_0\displaystyle\int_{y_\delta}^{y}[q(y)]^{\frac{1}{2}}\,dy+\frac{1}{4}\pi\right]}{[q(y)]^{\frac{1}{4}}} & \text{for} \quad y > y_\delta, \quad k_0\delta\to\infty, \quad (3.36a) \\ \dfrac{\exp\left(-ik_0\displaystyle\int_{y_\delta}^{y}[q(y)]^{\frac{1}{2}}\,dy\right)}{[q(y)]^{\frac{1}{4}}} & \text{for} \quad y < y_\delta, \quad k_0\delta\to\infty, \quad (3.36b) \end{cases}$$

provided that we choose the branch of the square root such that $q^{\frac{1}{2}} = i|q^{\frac{1}{2}}|$ when $q < 0$. Then since in both cases Π_+ represents an outgoing wave when $y\to+\infty$ and Π_- represents an outgoing wave when $y\to-\infty$ we can, in view of (2.28) and (3.27), put

$$P_U = D\Pi_+, \quad P_L = D\Pi_- \tag{3.37}$$

and

$$V_U \sim \frac{1}{i\rho_0 c_0 k_0}\Pi'_+, \quad V_L \sim \frac{1}{i\rho_0 c_0 k_0}\Pi'_-. \tag{3.38}$$

Inserting (3.34)–(3.36) into (3.37) and (3.38) and using the results in (3.5), we find that

$$\kappa_-(k_1|k_3)/\kappa_+(k_1|k_3) = \{[1-\tilde{k}_1 M(0)]^2 - \tilde{k}_1^2 - \tilde{k}_3^2\}^{\frac{1}{2}}/2\rho_0 c_0 D(0) \tag{3.39}$$

when there is no turning point or when the turning point lies above the plate, i.e. when $y_\delta > 0$. The expression for κ_-/κ_+ becomes considerably more complicated when y_δ lies below the plate and the indicated factorization (i.e. the determination of κ_+ and κ_-) leads to expressions involving singular integrals that must be evaluated numerically. In any case we shall show that this situation occurs over only a relatively small portion of the sound field when the Mach number is not too high and we shall not consider it further.

In the present case κ_+ can be found by factorizing (3.39) to obtain

$$\kappa_+ = \left\{k_0\frac{M_0+[1-(1-M_0^2)\tilde{k}_3^2]^{\frac{1}{2}}}{M_0+1}+(1-M_0)k_1\right\}^{-\frac{1}{2}},$$

where we have put $M_0 \equiv M(0)$. Finally inserting this together with (3.34)–(3.38) into (3.11) and (3.15), we obtain for the *leading edge*

$$T_{le} \sim \frac{\rho_0 c_0 M(\eta)}{1-M(\eta)\cos\theta_0}\left(\frac{Q(0)}{Q(\infty)}\right)^{\frac{1}{2}} \times \frac{\exp\left(ik_0\displaystyle\int_0^\infty [Q(y)-Q(\infty)]\,dy\right)}{[B_-(\cos\theta)-(1+M_0)\cos\theta_0]^{\frac{1}{2}}\,[B_+(\cos\theta)+(1-M_0)/M(\eta)]^{\frac{1}{2}}} \tag{3.40}$$

and for the *trailing edge*

$$T_{te} \sim \frac{-\rho_0 c_0 (M(\eta) - M_0)}{[1 - M(\eta)\cos\theta_0](1 - M_0\cos\theta_0)} \left(\frac{Q(0)}{Q(\infty)}\right)^{\frac{1}{2}} \times \frac{\exp\left(ik_0 \int_0^\infty [Q(y) - Q(\infty)]\, dy\right)}{[B_+(\cos\theta) + (1 - M_0)\cos\theta_0]^{\frac{1}{2}} [B_-(\cos\theta) - (1 + M_0)/M(\eta)]^{\frac{1}{2}}}, \tag{3.41}$$

where we have put

$$\left.\begin{aligned} Q(y) &= \{[1 - M(y)\cos\theta_0]^2 - \cos^2\theta_0 - \cos^2\theta\}^{\frac{1}{2}}, \\ B_\pm(\cos\theta) &= \{\pm M_0 + [1 - (1 - M_0^2)\cos^2\theta]^{\frac{1}{2}}\}/(1 \pm M_0). \end{aligned}\right\} \tag{3.42}$$

As we did in the low frequency case, we can now use these results together with (3.10) to show that the directivity patterns of the mean-square acoustic pressures in the plane of the plate (where $\theta = \frac{1}{2}\pi$ and $\theta_0 = \phi$) are given by

$$\frac{\sin\phi}{[1 - M(y_c)\cos\phi]^2} \left[\frac{1 + (1 - M_0)\cos\phi}{|1 - (1 + M_0)\cos\phi|}\right]^{\frac{1}{2}} \quad \text{for a leading edge with} \quad \phi > \cos^{-1}(1 + M_{\max})^{-1}, \tag{3.43}$$

$$\frac{\sin\phi}{[1 - M(y_c)\cos\phi]^2 [1 - M_0\cos\phi]^2} \left[\frac{|1 - (1 + M_0)\cos\phi|}{1 + (1 - M_0)\cos\phi}\right]^{\frac{1}{2}} \quad \text{for a trailing edge with} \quad \phi > \cos^{-1}(1 + M_{\max})^{-1}, \tag{3.44}$$

where $M_{\max}$ is the maximum Mach number in the shear layer.

These formulae must be multiplied by the exponential damping factor

$$\exp\left(-2k_0 \int_0^{y_\delta} \{\cos^2\phi - [1 - M(y)\cos\phi]^2\}^{\frac{1}{2}}\, dy\right)$$

when $0 \leqslant \phi \leqslant \cos^{-1}[(1 + M_0)^{-1}]$. They are invalid in the range

$$\cos^{-1}[(1 + M_0)^{-1}] < \phi < \cos^{-1}[(1 + M_{\max})^{-1}],$$

since the turning points will then lie below the plate and the present solution will not apply.

Thus the boundary of the zone of silence occurs at $\phi = \cos^{-1}(1 + M_0)^{-1}$. The turning point is then at the position of the plate. As ϕ increases the turning point moves below the plate and the solution becomes invalid. In this region the sound generated by the plate can be reflected by the shear layer, causing complicated interference effects. Finally, no turning points will occur in the range

$$\cos^{-1}(1 + M_{\max})^{-1} < \phi \leqslant \pi.$$

Equations (3.43) and (3.44) again respectively reduce to the $\cos^2\frac{1}{2}\phi$ and $\cos^2\frac{1}{2}(\pi - \phi)$ directivity patterns implied by the Ffowcs Williams & Hall result when the mean-flow Mach number goes to zero. These results are compared with each other and with the Ffowcs Williams & Hall result (oriented relative to the leading-edge configuration) in figure 7, where for purposes of illustration we have put $M(y_c) = M_0 = M_{\max}$. In evaluating the refraction integral, which appears in the zone of silence, we use the mean velocity field described in the next section. The leading-edge directivity patterns are seen to be fairly close to the Ffowcs Williams & Hall (1970) result even at relatively

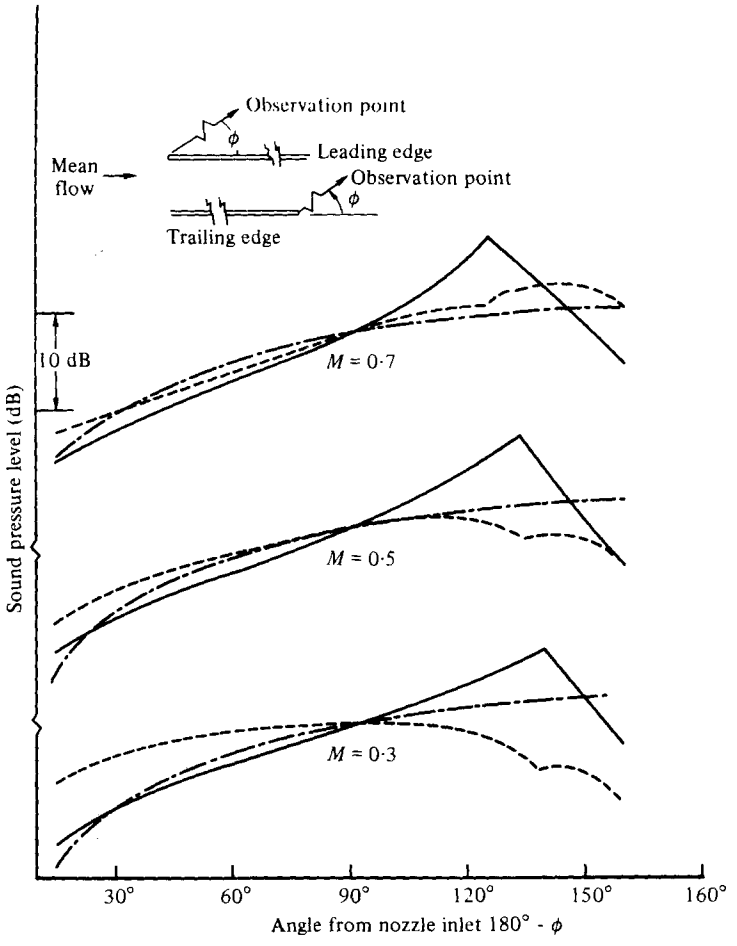

FIGURE 7. Comparison of leading- and trailing-edge radiation patterns in high frequency limit. ——, leading edge; – – –, trailing edge; — · —, Ffowcs Williams & Hall (oriented relative to leading-edge configuration).

large Mach numbers. Thus, as one might expect, the mean flow 'shields' the gust from the stationary fluid at infinity and thereby eliminates the convective amplification due to the relative motion of the incident disturbance and the stationary fluid. But the mean flow alters the trailing-edge radiation patterns in a very remarkable way. It causes these patterns to approach that of a leading edge with the same mean-flow direction rather than being the mirror image (about $\phi = \frac{1}{2}\pi$) of that pattern as the Ffowcs Williams & Hall (1970) theory would predict. When the Mach number approaches zero the trailing-edge radiation pattern approaches the expected $\sin^2\frac{1}{2}\phi$ pattern, which is the mirror image of the $\cos^2\frac{1}{2}\phi$ pattern shown in the figure.

3.5. *Behaviour of solutions at the edges*

The Wiener–Hopf solutions to the scattering problems are not unique. However, they can be made unique by specifying their behaviour at the (leading or trailing) edges. In carrying out the analysis we have always sought the solutions with the weakest

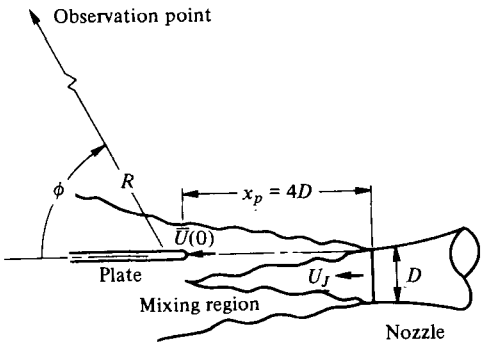

FIGURE 8. Configuration of plate experiment. Nozzle diameter $D = 4$ in.; distance to observation point $R = 15$ ft.

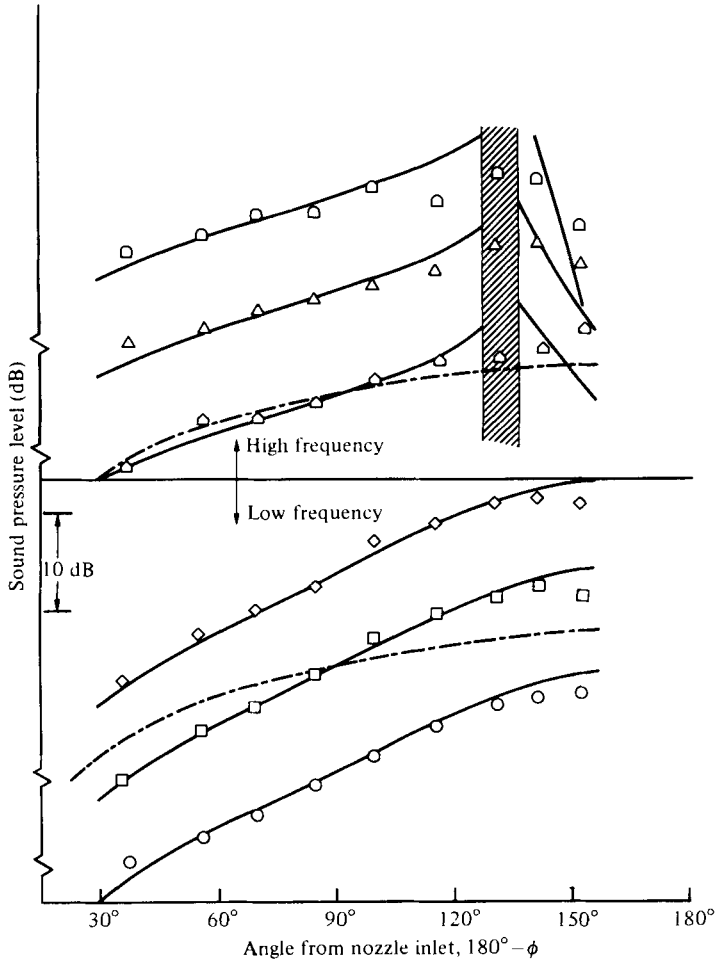

FIGURE 9. Shape of one-third octave radiation patterns for $U_J = 700$ ft/s.
——, shear-layer theory; — · —, $\cos^2 \frac{1}{2}\phi$.

Experiment	∩	△	⌂	◇	□	○
Cycles	6500	2500	1600	630	500	400

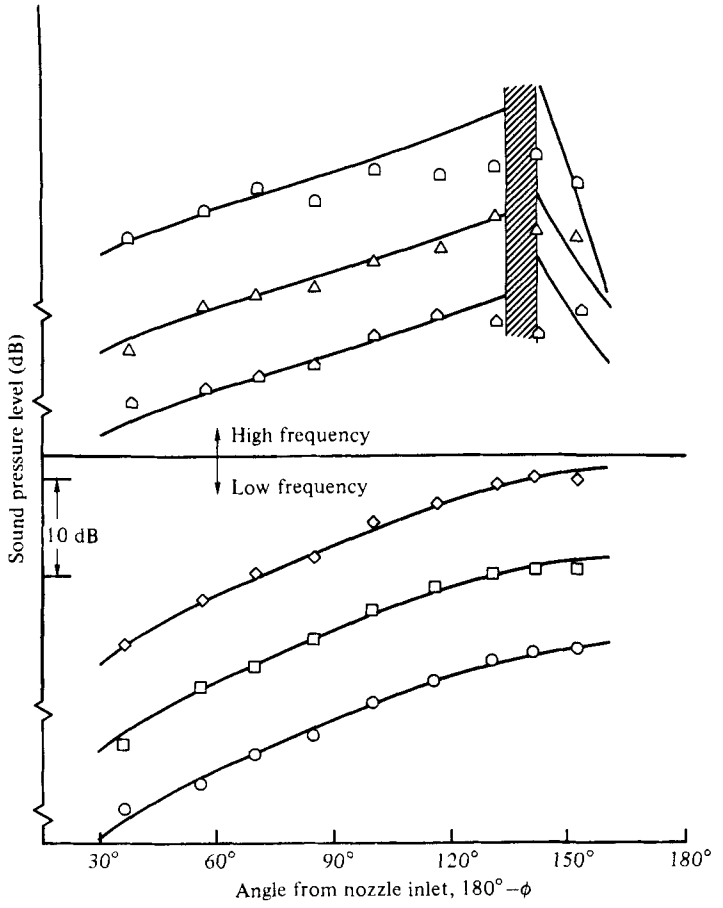

FIGURE 10. Shape of one-third octave radiation patterns for $U_J = 500\,\text{ft/s}$. Notation as in figure 9.

singularities at these points. However, it is rather difficult to prove that this will ensure that the trailing-edge solution will always satisfy a Kutta condition. But the results of appendix C show that this does occur for both the high and the low frequency solution. In fact it is shown in both these cases that, as usually happens when there is a mean flow, the pressure jump across the plate goes to zero like $x^{\frac{1}{2}}$ as $x \to 0$.

The results of this appendix also show that pressure fluctuations produced at an upstream edge exhibit the expected $x^{-\frac{1}{2}}$ singularity at that edge when $k_0\delta \gg 1$. But the singularity disappears when $k_0\delta \to 0$ and the pressure jump goes to zero like $x^{\frac{3}{2}}$ as $x \to 0$.

3.6. *Comparison with experiment*

In order to verify the directivity patterns deduced in the preceding sections these results are compared with the one-third octave sound pressure levels produced by a large flat plate in a turbulent jet, which were measured by Olsen (1976). The plate was positioned parallel to the jet axis with its leading edge centred in the mixing region 4 diameters downstream of the nozzles as shown in figure 8. The relevant geometric parameters are indicated on the figure.

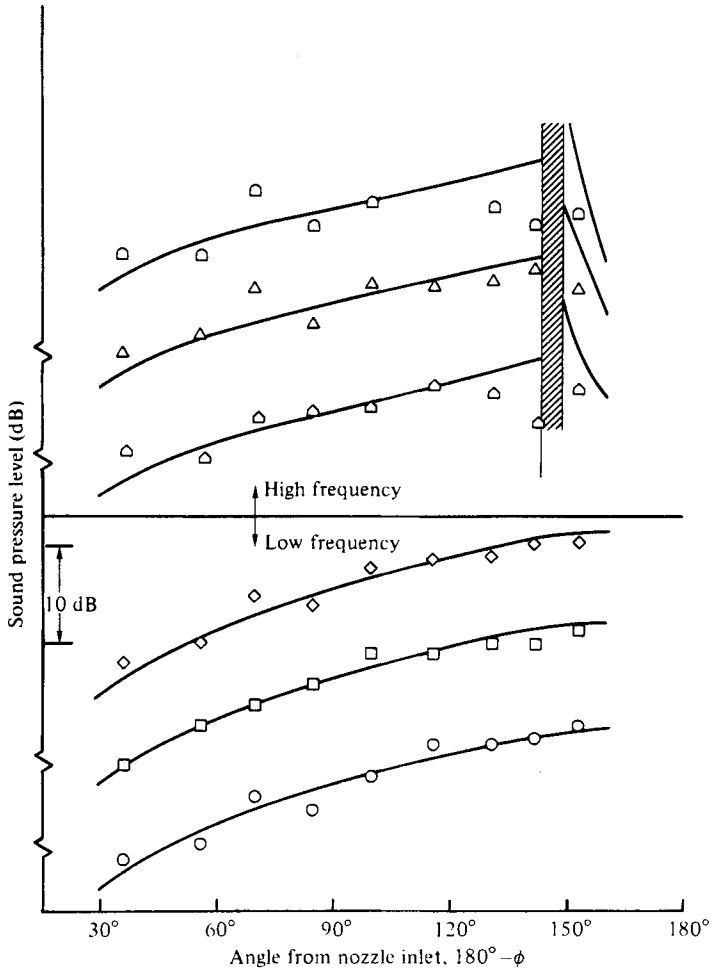

FIGURE 11. Shape of one-third octave radiation patterns for $U_J = 300$ ft/s. Notation as in figure 9.

As in the case where the mean flow is uniform, the scattering of the turbulence will be completed in a relatively short streamwise distance. We therefore suppose that the incident turbulence can be represented by the gust solution of the previous section. We shall not consider the possible effect of any instability wave solutions that may appear in the representation of the *incident* turbulence, primarily because we feel that they are irrelevant to turbulent scattering problems. Since the most intense turbulence is at the centre of the mixing region, where the plate is located, we set y_c equal to the plate position $y = 0$. Then the mean flow velocity at this position is approximately 0·615 times the jet velocity U_J.

The mean velocity profiles must be specified in the region between the plate and the observer in order to calculate the refraction integrals that multiply the high frequency solutions in the zone of silence. It was shown by Townsend (1956, p. 176) that the velocity profiles in this outer portion of the mixing layer can be fitted quite

well by $\overline{U}(y)/U_J = \frac{1}{2}[1-\tanh(ay-b)]$. We chose the constants a and b to make $\overline{U}(0) = 0{\cdot}615U_J$ and (Davies, Fisher & Barratt 1963)

$$\frac{D}{U_J}\overline{U}'(0) = -6/(x_p/D+0{\cdot}4),$$

where, as indicated in figure 8, x_p is the distance between the edge of the plate and the nozzle and D is the diameter of the nozzle.

The one-third octave radiation patterns in the plane perpendicular to the plate are compared with the theoretical predictions in figures 9–11. The levels of the theoretical curves are adjusted to go through the data at approximately 90°. Results are presented for three different jet velocities and six frequencies. Each figure contains three curves in the low frequency range and three in the high.

The minimum value of the frequency is limited by the requirement that the plate be long compared with the wavelength (since it is assumed in the analysis that the plate is semi-infinite). At the lowest frequency shown the 8 ft plate used in the experiment is approximately three wavelengths long. The upper limit of the low frequency range is dictated by the requirement that the wavelength be large compared with the jet diameter, or at least the thickness of jet through which the sound must pass.

The inverse requirement sets the lower limit of the high frequency range. The highest frequency used was the maximum value consistent with the requirement that the acoustic levels be well above the background jet noise in the frequency band under consideration.

The agreement between theory and experiment is seen to be quite good in the low frequency range especially at the highest two velocities, where the data exhibit much less scatter than they do at 91·5 m/s. Also shown (on figure 9) is the $\cos^2\frac{1}{2}\phi$ directivity pattern found by Ffowcs Williams & Hall (1970) for a leading edge in free space. It can be seen that the effects of the Doppler factors are substantial even at the relatively low velocities of the present experiments.

In the high frequency range the agreement is fairly good at the lowest two frequencies but not at the highest. This is probably due to the turbulent scattering and related effects that must occur when the wavelength of the sound becomes comparable to the turbulent eddy size. It could also reflect the fact that the wavelength is no longer small compared with the plate thickness.

In each figure the shaded region corresponds to the range of angles where the high frequency solutions are invalid. The zone of silence lies to the right of this region. At the highest jet velocity of 213 m/s there are two sets of data points within the zone of silence. The leftmost of these lie fairly close to the theoretical curves but those on the right are substantially higher. This is probably again due to turbulent scattering. The free-space theory of Ffowcs Williams & Hall is also plotted. It can be seen that it is fairly close to the high frequency theory at all points outside the zone of silence.

4. Concluding remarks

It is shown that the pressure and velocity fluctuations of the unsteady motion on a transversely sheared mean flow can be calculated by differentiation from a certain potential which satisfies an inhomogeneous wave equation. This representation explicitly exhibits two convected quantities which are associated with the upstream

vorticity field and are shown to 'drive' the gust-like or 'hydrodynamic' motion on the sheared mean flow. It is used to study the interaction of an unsteady shear flow with a semi-infinite plate. The acoustic field produced by this interaction is calculated in the low and high frequency limits and the results are compared with experimental one-third octave directivity patterns. The agreement is fairly good at high frequencies and remarkably good at low frequencies.

The author would like to thank Dr Theodore Fessler for carrying out the numerical computations and Dr W. A. Olsen for supplying additional experimental data that did not appear in his published report. Thanks are also due to Dr Olsen for helpful discussions about the measurements.

Appendix A

In this appendix we show that the results of this paper agree with those of I when the motion is two-dimensional. The difference between equation (2.38) of this paper and equation (3.27) of I is primarily due to the fact that we chose to express the results in terms of different linearly independent homogeneous solutions to the governing ordinary differential equations. Thus the $\pm\infty$ outgoing-wave solutions of this paper, P_U and P_L respectively, are related to the outgoing-wave solution P_o of I by

$$P_o(\alpha, y) = \begin{cases} a_+(\alpha)\, P_U(k_1, y) & \text{for} \quad y > 0, \\ a_-(\alpha)\, P_L(k_1, y) & \text{for} \quad y < 0, \end{cases}$$

where the $a_\pm(\alpha)$ are constants.

In fact if we let U be the amplitude of the axial gust velocity u_g (i.e. if we let U be related to u_g in the same way as P is related to p_g and V is related to v_g) we can write

$$\mathbf{Z}_o(\alpha, y) = \left\{ \begin{matrix} a_+(\alpha)\, \mathbf{Z}_U(k_1, y) & \text{for} \quad y > 0, \\ a_-(\alpha)\, \mathbf{Z}_L(k_1, y) & \text{for} \quad y < 0, \end{matrix} \right\} \tag{A 1}$$

where $\mathbf{Z}_o$ is defined by equation (3.9) of I and $\mathbf{Z}_U$ and $\mathbf{Z}_L$ are similarly defined by

$$\mathbf{Z}_\lambda = \{P_\lambda, V_\lambda, U_\lambda\} \quad \text{for} \quad \lambda = U, L. \tag{A 2}$$

Then since $\mathbf{Z}_1$ and $\mathbf{Z}_o$ of I are linearly independent (i.e. since P_1 and P_o are linearly independent etc.), there must exist constants $b_\pm(\alpha)$ and $c_\pm(\alpha)$ such that

$$\mathbf{Z}_L(k_1, y) = b_+(\alpha)\, \mathbf{Z}_o(\alpha, y) + c_+(\alpha)\, \mathbf{Z}_1(\alpha, y) \quad \text{for} \quad y > 0 \tag{A 3}$$

and

$$\mathbf{Z}_U(k_1, y) = b_-(\alpha)\, \mathbf{Z}_o(\alpha, y) + c_-(\alpha)\, \mathbf{Z}_1(\alpha, y) \quad \text{for} \quad y < 0. \tag{A 4}$$

These formulae relate the solutions employed in this paper to those used in I. But since $\mathbf{Z}_U$ and $\mathbf{Z}_L$ represent continuous solutions in this paper while the solutions $\mathbf{Z}_o$ and $\mathbf{Z}_1$ of I are in general discontinuous across $y = 0$ we must have

$$a_\pm^{-1}\, P_o(\alpha, 0\pm) = b_\mp\, P_o(\alpha, 0\mp) + c_\mp\, P_1(\alpha, 0\mp)$$

and

$$a_\pm^{-1}\, V_o(\alpha, 0\pm) = b_\mp\, V_o(\alpha, 0\mp) + c_\mp\, V_1(\alpha, 0\mp),$$

which can be solved for $a_\pm$ and $b_\pm$ to obtain

$$b_\pm = -\,\Gamma_\pm^+\, c_\pm, \quad a_\pm^{-1} = \Gamma_\pm^-\, c_\mp, \tag{A 5}$$

where the Γ's are defined in equation (3.16) of I.

Now it follows from equation (3.2*b*) of I that

$$\begin{aligned}\mathcal{J}(k_1,\eta) &\equiv \overline{U}'[P_L(k_1,\eta)\,V_U(k_1,\eta)-P_U(k_1,\eta)\,V_L(k_1,\eta)]/i(\omega-\overline{U}k_1)\\ &= P_L(k_1,\eta)\,U_U(k_1,\eta)-P_U(k_1,\eta)\,U_L(k_1,\eta).\end{aligned}$$

Hence it follows from (A 1)–(A 4) that

$$\mathcal{J}(k_1,\eta) = \pm\frac{c_\pm(\alpha)}{a_\pm(\alpha)}\left[\frac{P_1(k_1,\eta)}{P_o(k_1,\eta)}\frac{U_o(k_1,\eta)}{U_1(k_1,\eta)}-1\right]U_1(k_1,\eta)\,P_o(k_1,\eta) \quad \text{for} \quad \eta \gtrless 0.$$

Then, using equations (3.4) and (3.5) of I together with the fact that P_o is a linear combination of P_1 and P_2 etc., we find that

$$J(\eta) \equiv \lim_{k_1\to\omega/\overline{U}(\eta)} \mathcal{J}(k_1,\eta) = \mp\frac{c_\pm(\omega/\overline{U})}{a_\pm(\omega/\overline{U})}\,U_1(\omega/\overline{U},\eta)\,P_o(\omega/\overline{U},\eta). \tag{A 6}$$

Finally inserting (A 1)–(A 6) into (2.38), we obtain the second component (i.e. the v_g component) of equation (3.27) of I. This same procedure can of course be used to obtain the other components of the latter equation.

Appendix B

In this appendix ω_c is related to the physical flow variables. The ζ and x components of the fluctuating vorticity $\boldsymbol{\omega} = \nabla\times\mathbf{u}$ are given by

$$\omega_\zeta = \frac{\partial v}{\partial x}-\frac{1}{g}\frac{\partial u}{\partial \eta}, \quad \omega_x = \frac{1}{hg}\left[\frac{\partial}{\partial\eta}(hw)-\frac{\partial}{\partial\zeta}(gv)\right].$$

Inserting (2.9) and using (2.10), (2.13) and (2.14) to eliminate the highest derivatives of ϕ with respect to x and t, we get

$$\omega_\zeta = \omega_c-\frac{\overline{U}'}{g}\frac{p}{\rho_0 c_0^2}-\frac{\overline{U}'}{hg^2}\frac{\partial}{\partial\zeta}\left(\frac{g}{h}\frac{\partial}{\partial\zeta}\frac{D\phi}{Dt}\right)+\left[\frac{h}{g}\frac{\partial}{\partial\eta}\left(\frac{\overline{U}'}{hg}\right)\right]\lambda-\frac{1}{g}\frac{\partial}{\partial\eta}\left(\frac{1}{hg}\frac{\partial}{\partial\zeta}\overline{U}'\theta\right)$$

and

$$\omega_x = -\frac{1}{hg}\frac{\partial}{\partial x}\left[\frac{\partial}{\partial\eta}\left(h\frac{\overline{U}'}{g}\theta\right)+\overline{U}'\frac{\partial}{\partial\zeta}\frac{D\phi}{Dt}\right],$$

where we have put

$$\lambda \equiv \frac{1}{g}\left(\frac{\partial}{\partial\eta}\frac{D\phi}{Dt}+2\overline{U}'\frac{\partial\phi}{\partial x}\right). \tag{B 1}$$

Eliminating $D\phi/Dt$ between these equations gives

$$\frac{\partial\omega_c}{\partial x}+\gamma = \frac{\partial}{\partial x}\left\{\omega_\zeta+\frac{\overline{U}'}{g}\frac{p}{\rho_0 c_0^2}-\left[\frac{h}{g}\frac{\partial}{\partial\eta}\left(\frac{\overline{U}'}{hg}\right)\right]\lambda\right\}-\frac{1}{g^2h}\frac{\partial}{\partial\zeta}(g^2\omega_x), \tag{B 2}$$

where we have put

$$\gamma = -\frac{1}{g}\frac{\partial}{\partial x}\left[\frac{\partial}{\partial\eta}\frac{1}{hg}\frac{\partial}{\partial\zeta}-\frac{1}{hg}\frac{\partial}{\partial\zeta}\frac{g}{h}\frac{\partial}{\partial\eta}\frac{h}{g}\right]\overline{U}'\theta = \frac{\overline{U}'}{hg^2}\frac{\partial}{\partial x}\left[\theta\frac{\partial^2}{\partial\zeta\partial\eta}\ln(h/g)+\frac{2}{h}\frac{\partial h}{\partial\eta}\frac{\partial\theta}{\partial\zeta}\right]. \tag{B 3}$$

Appendix C

It follows from (3.4)–(3.6) that the pressure jump Δp across a plate that extends to infinity in the downstream direction is given by

$$\Delta\tilde{p}(x,z) = \int_{-\infty}^{-\infty}\int_{-\infty}^{\infty} \exp(ik_3 z)\,\bar{\Omega}(\eta|k_3)\,\mathscr{K}_v(0|\eta,k_3)\,\mathscr{R}(x|\eta,k_3)\,d\eta\,dk_3, \tag{C 1}$$

where

$$\mathscr{R}(x|\eta,k_3) = \mathscr{R}_{le}(x|\eta,k_3) = \frac{\bar{U}(\eta)}{2\pi i}\int_{-\infty}^{\infty} \frac{\exp(ik_1 x)\,\kappa_+(\omega/\bar{U}(\eta)|k_3)}{[\omega-k_1\bar{U}(\eta)]\,\kappa_-(k_1|k_3)}\,dk_1. \tag{C 2}$$

For a trailing edge the pressure jump across the plate is still given by (C 1) but with

$$\mathscr{R}(x|\eta,k_3) = \mathscr{R}_{te}(x|\eta,k_3) = \frac{\bar{U}(\eta)}{2\pi i}\int_{-\infty}^{\infty} \frac{\exp(ik_1 x)\,\kappa_+(k_1|k_3)\,dk_1}{[\omega-k_1\bar{U}(\eta)]\,\kappa_-(\omega/\bar{U}(\eta)|k_3)}. \tag{C 3}$$

It follows from (3.16)–(3.19) that

$$\mathscr{R}_{le}(x|\eta,k_3) = -\frac{\rho_0\omega^2\bar{U}(\eta)}{\pi[\omega/\bar{U}(\eta)+\lambda_0]^{\frac{1}{2}}}\int_{-\infty}^{\infty} \frac{\exp(ik_1 x)\,dk_1}{[\omega-k_1\bar{U}(\eta)]\,[\omega-k_1\bar{U}(0)]\,(k_1-\lambda_0)^{\frac{1}{2}}} \quad \text{for} \quad k_0\delta \ll 1 \tag{C 4}$$

and

$$\mathscr{R}_{te}(x|\eta,k_3) = \frac{\rho_0\omega\bar{U}^2(\eta)}{\pi[\omega/\bar{U}(\eta)-\lambda_0]^{\frac{1}{2}}\,[\bar{U}(0)-\bar{U}(\eta)]}\int_{-\infty}^{\infty} \frac{\exp(ik_1 x)\,dk_1}{[\omega-k_1\bar{U}(\eta)]\,(k_1+\lambda_0)^{\frac{1}{2}}} \quad \text{for} \quad k_0\delta \ll 1, \tag{C 5}$$

where $\lambda_0 \equiv (k_0^2-k_3^2)^{\frac{1}{2}}$. Since the integrands of (C 4) and (C 5) respectively behave like $k_1^{-\frac{1}{2}}$ and $k_1^{-\frac{3}{2}}$ as $k_1\to\infty$, it follows from the theory of Fourier transforms that

$$\mathscr{R}_{le}(x|\eta,k_3) \sim x^{\frac{3}{2}}, \quad \mathscr{R}_{te}(x|\eta,k_3) \sim x^{\frac{1}{2}} \quad \text{as} \quad x\to 0 \quad \text{for} \quad k_0\delta \ll 1.$$

Similarly we find upon inserting (3.39) together with the equation for κ_+ into (C 2) and (C 3) that

$$\mathscr{R}_{le}(x|\eta,k_3) \sim x^{-\frac{1}{2}}, \quad \mathscr{R}_{te}(x|\eta,k_3) \sim x^{\frac{1}{2}} \quad \text{as} \quad x\to 0 \quad \text{for} \quad k_0\delta \gg 1.$$

REFERENCES

ABRAMOWITZ, M. & STEGUN, I. 1964 *Handbook of Mathematical Functions*. Washington: Nat. Bur. Stand.

DAVIES, P. O. A. L., FISHER, M. J. & BARRATT, M. J. 1963 The characteristics of the turbulence in the mixing region on a round jet. *J. Fluid Mech.* **15**, 337.

DOWLING, A. P., FFOWCS WILLIAMS, J. E. & GOLDSTEIN, M. E. 1978 Sound production in a moving stream. *Phil. Trans. Roy. Soc.* A **288**, 321.

DURBIN, P. 1979 Rapid distortion for turbulence distorted by a constant shear-layer adjacent to a wall. Submitted to *J. Fluid Mech.*

FFOWCS WILLIAMS, J. E. & HALL, H. H. 1970 Aerodynamic sound generation by turbulent flow in the vicinity of a scattering half plane. *J. Fluid Mech.* **40**, 657.

GOLDSTEIN, M. E. 1975 The low frequency sound from multiple sources in axisymmetric shear flows, with application to jet noise. *J. Fluid Mech.* **70**, 595.

GOLDSTEIN, M. E. 1976 *Aeroacoustics*. McGraw-Hill.

GOLDSTEIN, M. E. 1978 Characteristics of the unsteady motion on transversely sheared mean flows. *J. Fluid Mech.* **84**, 305.

HUNT, J. C. R. 1977 A review of the theory of rapidly distorted flows and its applications. *13th Biennial Fluid Dyn. Symp., Poland.* (To be published in *Fluid Dyn. Trans., Polish Acad. Sci.*)

KOVÁSZNAY, L. S. G. 1953 Turbulence in supersonic flow. *J. Aero Sci.* **20**, 657.

LIEPMANN, H. W. 1952 On the application of statistical concepts to the buffeting problem. *J. Aero. Sci.* **19**, 793.

LIGHTHILL, M. J. 1952 On sound generated aerodynamically. I. General theory. *Proc. Roy. Soc.* A **211**, 564.

MANI, R. 1976 The influence of jet flow on jet noise. Part 1. The noise of unheated jets. *J. Fluid Mech.* **73**, 753.

MOFFATT, H. K. 1965 The interaction of turbulence with strong wind shear. *Proc. URSI–IUGG Int. Coll. Atmos. Turb. Radio Wave Propagation, Moscow.*

MÖHRING, W. 1976 Über Schallwellen in Scherströmungen, Fortschritte der Akustik. *DAGA* 76, *VDI*, pp. 543–546.

MÖRSE, P. M. & FESHBACH, H. 1953 *Methods of Theoretical Physics.* McGraw-Hill.

OLSEN, W. A. 1976 Noise generated by impingement of turbulent flow on airfoils of varied chord, cylinders and other flow obstructions. *N.A.S.A. Tech. Memo.* X-73644. (See also *3rd A.I.A.A. Aero-Acoustics Conf. A.I.A.A. Paper* no. 76-504.)

SEARS, W. R. 1941 Some aspects of non-stationary airfoil theory and its practical applications. *J. Aero. Sci.* **83**, 104.

TOWNSEND, A. A. 1956 *The Structure of Turbulent Shear Flow.* Cambridge University Press.

WILLS, J. A. B. 1964 On convection velocities in turbulent shear flows. *J. Fluid Mech.* **20**, 417.